Medical isotope production using Lighthouse accelerator

J.W. Blokker

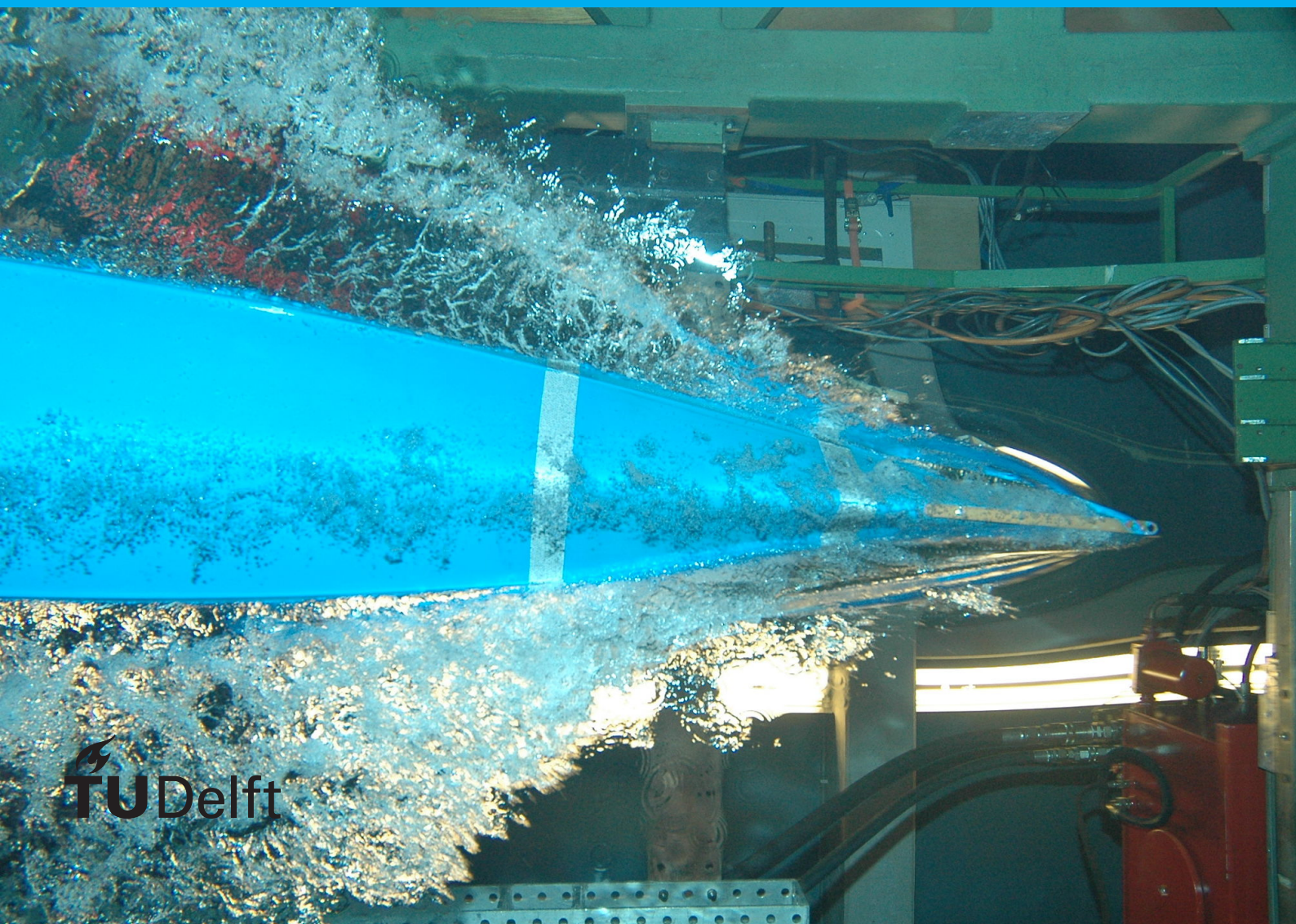

Medical isotope production using Lighthouse accelerator

by

J.W. Blokker

to obtain the degree of

Bachelor of Science in Applied Physics

at the Delft University of Technology,
to be defended on Wednesday November 1, 2017 at 02:00 PM.

Student number:	4306120	
Project duration:	April 24, 2017 – November 1, 2017	
Thesis committee:	Prof. dr. ir. J.L. Kloosterman,	TU Delft, supervisor
	Dr. ir. M. Rohde,	TU Delft
	Dr. ir. P. de Jager	ASML

An electronic version of this thesis is available at http://repository.tudelft.nl/.

TU Delft

Abstract

The number of new cancer cases unfortunately increases each year and is expected to grow to 23.6 million in 2030. In order to treat all these new cases new and cheaper ways of fighting cancer are needed. One method that is becoming more popular is the use of medical isotopes that emit radiation which destroys the tumor. Many of these isotopes are produced in specialized nuclear reactors. There are only a handful of these reactors in the world, making production expensive and resulting in a limited production capacity. A new way of producing these isotopes would be to use ASML's Lighthouse accelerator, which uses electron beams to create radioactive molybdenum isotopes for medical research, emitting neutrons in the process.

The goal of this thesis was to investigate if the neutrons emitted from the molybdenum could be used to create more medical isotopes. Two isotopes were chosen to be studied; ^{166}Ho and ^{177}Lu. Lutetium needs no special preparation before irradiation, but in order to use radioactive holmium atoms for cancer treatment they have to be placed in special lactic acid microspheres. The placement of the holmium atoms in the microspheres happens before irradiation.

This research was done using Serpent, a program specifically designed for modeling nuclear reactors. Using two different geometries, the neutron absorption in the targets was studied. The first geometry consisted of a spherical molybdenum core surrounded by multiple spherical layers. The second geometry of a cylindrical molybdenum core with multiple cylindrical layers around it with a final spherical layer.

The results showed that due to its high required specific activity ^{177}Lu could not be produced within the allowed time frame. For ^{166}Ho, however, it was possible. If ^{166}Ho with a high enough specific activity was to be produced within the allowed time frame a minimum neutron absorption of 0.21% was needed. In the second geometry, which resembled the real design more closely, the maximum absorption reached with additional modification of the geometry was approximately 1.25%, well above what is needed. When a tungsten gamma shield with a thickness of approximately 8.5 cm was added to this geometry the neutron absorption was roughly 0.70%, while almost all primary gamma radiation was shielded. The purpose of the gamma shield was to gamma dose rate of the microspheres, which can cause structural disintegration. It can be concluded that using the neutrons emitted from the molybdenum core can be used to produce medical isotopes.

Contents

List of Figures

List of Tables

Nomenclature

Symbols

Symbol	Description	Units
SA	specific activity	Bq·g⁻1 (1 Ci = 37·10^9 Bq)
$t_{1/2}$	half-life	s
ρ	Density	g·cm^{-3}
σ	microscopic cross-section	b (1 b = 10^{-24} cm^2)
Σ	macroscopic cross-section	cm^{-1}
A_d	atomic number density	cm^{-3}
ν	neutron speed	cm·s^{-1}
F	reaction-rate density	cm^{-3}·s^{-1}
ϕ	neutron flux	cm^{-2}·s^{-1}
ξ	lethargy gain	-
N_r	number of radioactive atoms	-
λ	decay constant	s^{-1}
χ	neutrons absorbed in the target atoms per second	s^{-1}
A_f	gamma attenuation factor	-
B	buildup factor	-
μ	linear attenuation coefficient	cm^{-1}
R_1	molybdenum target radius	cm
R_2	moderator/gamma shield radius	cm
R_3	Ho or Lu target radius	cm
R_4	reflector radius	cm
R_5	absorption layer radius	cm
V	volume of Ho or Lu target	cm^3
W	width of the Ho or Lu target in the cylindrical geometry	cm

Acronyms

Acronym	Meaning
SPECT	single-photon emission computed tomography
HCC	hepatocellular carcinoma
PLLA-MS	poly(L-lactic acid) microspheres
HoAcAc	holmium acetylacetonate
MRI	magnetic resonance imaging

1 Introduction

In 2012 an estimated number of 12.1 million new cases of cancer occurred worldwide and 8.2 million people died as a result of cancer [19]. The number of people diagnosed with cancer each year is expected to grow to 23.6 million worldwide by 2030 [19]. Contrary to popular belief, cancer is not a welfare disease that mostly targets older, wealthy people living in developed countries. In 2008, over 55% of all deaths related to cancer occurred in less developed regions on the planet [4]. Therefore, new and cheaper ways of diagnosing and fighting cancer are needed in order to combat this increase in people suffering from cancer. It is, however, not only beneficial for developing countries to develop new methods of treating cancer. Cancer remains, despite scientific progress, a major cause of death in ages 40 or older. Between 1950 and 2005, the death rate of cancer in the U.S., adjusted for population size and age, only dropped 5% [11] and many forms of cancer, such as pancreatic, remain largely incurable, despite billions having been invested in research. As such it is crucial, in face of a population with an increasing average age, that the death rate of cancer is decreased. One method of diagnosing or treating cancer that is becoming more and more popular is the use of medical isotopes. This method uses radioactive particles that are directly injected into the body and can be placed very close to the diseased tissue.

1.1. Diagnosis and treatment using medical isotopes

Every year an estimated 48 million studies and treatments are done worldwide using medical isotopes [16]. In most of these cases, around 80%, technetium-99m is used. This is a medical isotope produced in a couple of nuclear reactors around the world. This isotope is used for diagnostic purposes as the gamma rays emitted as the technetium atoms decay is used the create a image of (a certain part) of the body using SPECT [16]. Besides diagnosis, medical isotopes also can be used for therapy. Therapy with isotopes can be subdivided in two categories: nuclear medicinal therapy and palliative therapy. Nuclear medicinal therapy focuses on destroying a specific tissue, while palliative therapy focuses on pain relief, increasing quality of life. A major benefit of these therapies is that they can be very personalized. As a result, treatment is much more effective and unnecessary collateral damage can be prevented. Furthermore, combining diagnosis and therapy is an emerging application of medical isotopes. By labeling a therapeutic isotope to a molecule labeled with a diagnostic isotope that has shown to be absorbed in the correct tissue the absorption pattern in the therapeutic treatment is guaranteed to be the same as in the diagnostic treatment. This results in an even more personalized treatment. At the moment, most of the isotopes used in therapy are produced in a handful of nuclear reactors around the world, which are all starting to approach the end of their life cycle. This means that supply is limited and isotopes generally have to be transported over long distances. At the moment there are different projects around the world trying to develop new ways of producing isotopes normally produced in nuclear reactors cheaper and more efficient. One of these projects is ASML's 'Lighthouse' project or the 'Lighthouse accelerator'. This device uses an electron accelerator to create high-energetic

photons which are used to irradiate a certain target and create a medical isotope. This use of this accelerator for the production of medical isotopes will be the focus of this research project.

1.2. Prior research

The Lighthouse reactor is still in early stages of development and at the moment only exists as a conceptual idea. Early analysis of the reactor shows that is is possible that this new way of producing isotopes results in little nuclear waste and is more cost-efficient than current methods of production [1]. In these early phases of development a material that has shown much promise as the target of the reactor is molybdenum-100. By irradiating molybdenum-100 with an electron beam molybdenum-99 is created by ejecting a neutron, which decays into technetium-99m, which is the most commonly used medical isotope in the world, as stated before. Besides neutrons photons are also ejected from the target. Bijers and Brandenburg [2] have, using FLUKA [3, 9], a program designed specifically for accelerator applications, calculated the neutron and photon spectra of the fields produced in the ^{100}Mo target. They used this data to calculate how thick the shielding walls should be and which material should be used to built them. There is, however, instead of simply capturing the neutrons and photons in the shields a second option. Just like in nuclear reactors, the neutron flux originating from the molybdenum target could be used to create medical isotopes. If this is possible it would be a waste not to do this, as the reactor likely becomes more cost-efficient and medical isotopes could become more readily available and cheaper.

1.3. Research goals and thesis overview

The goal of this research project is to find out if it is possible to use the neutron flux that radiates from the target to produce secondary medical isotopes and, when it is possible, to see if the production of these isotopes is high enough that this becomes a feasible method of producing them for medical purposes. In order to do this the focus of this research project will be on optimizing the neutron absorption in the isotope targets and therefore the isotope production rate. This will be done by examining multiple geometries using Serpent [12]. To optimize isotope production and to come to a conclusion about the possibility of secondary isotope production the following questions have to be answered:

- Which isotopes can be produced using this method?
- Which parameters influence the production rate of the isotopes?
- What should be the value of the relevant parameters?
- Which materials should be used in the geometry?
- What should be the shape of the geometry?
- What are the boundary conditions?

Two isotopes were chosen to be researched in this project: ^{166}Ho and ^{177}Lu. The reason these were chosen will be derived in the next chapter. The production of these isotopes is limited by the following boundary conditions: the required specific activity (SA) when the irradiation time is finished and the allowed irradiation time. These boundary conditions are displayed in table 1.1

Table 1.1: Boundary conditions for the production of ^{166}Ho and ^{177}Lu

Material	Required specific activity	irradiation time
^{166}Ho	4.4-7.4 Ci·g^{-1}	$3 \cdot t_{1/2,^{166}Ho}$
^{177}Lu	$19 \cdot 10^3$ Ci·g^{-1}	$3 \cdot t_{1/2,^{177}Lu}$

Furthermore, there is a boundary condition that only applies to ^{166}Ho, the absorption of gamma rays. The reason for this will be explained later in the report. At this point this

boundary condition is not quantifiable.

The other questions will be answered in the following chapters, of which the overview is as follows: in the second chapter the Lighthouse accelerator will be discussed more in detail as well as the medical isotopes chosen for this research. After that there will be a more in depth explanation of the neutron capture process. In the third chapter the different setup geometries used in this research project will be discussed. Next, in the fourth chapter, the numerical method using Serpent will be explained. In chapter 5 the results of these simulations will be presented and discussed and in chapter 6 a conclusion will be made as well as recommendations.

2

Theory

2.1. Lighthouse accelerator

2.1.1. Design of the Lighthouse

The Lighthouse accelerator was in the first stages of its development not meant to produce medical isotopes. Originally, it was supposed to be a new type of light source that ASML would use in the next version of their lithography machines. The electron beam would be sent through an undulator, which is a series of magnets, producing extreme ultra violet (EUV) light, that would be used to create microchips. However, it was also discovered that it was possible to create radioactive isotopes by hitting certain targets with the electron beam. A schematic overview of the Lighthouse accelerator is shown in figure 2.1

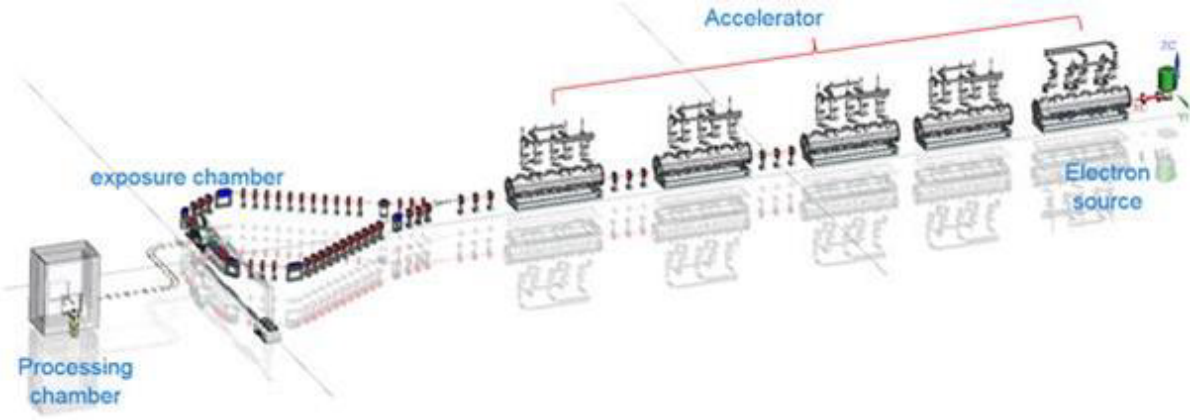

Figure 2.1: A schematic overview of the Lighthouse accelerator, total length 60 m [1].

The electrons are generated by a laser hitting a disk. After that, the electrons are accelerated in the linear accelerator. At the end of the accelerator the beam is split into two 60 MeV, 15 mA electron beams, with a combined power of 1.8 MW, which hit the first target from opposite sides. Because of the electrons losing energy, Bremsstrahlung photons are emitted from the first target. These photons then hit the second target, ejecting a neutron or a photon. Contrary to a conventional linear accelerator, which uses tungsten as the first target, the Lighthouse uses the same material for the first target as the second, which is molybdenum. In figure 2.2 the reaction process of the production of ^{99}Mo is shown.

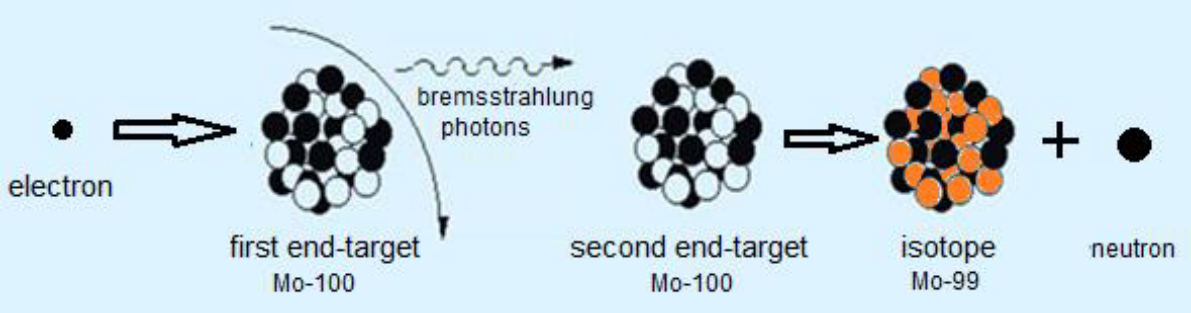

Figure 2.2: Production of ^{99}Mo with the Lighthouse reactor [1].

2.1.2. Neutron and photon spectra

Bijers and Brandenbrug [2] have calculated the neutron and photon spectra using FLUKA [3, 9]. In their simulations, however, only one electron beam was used to irradiate the target. The geometry used can be seen in figure 2.3. The electron beam impinges though a 0.3 mm thick SiC window after which it hits the ^{100}Mo target with density ρ = 5.128 gcm^{-3} and dimensions 30×30×56.6 mm, which gives it a volume of approximately 51 cm^3. The molybdenum target has 50% of the density of solid molybdenum because in the real setup the target consist of many slices perforated with microtubes. These microtubes allow the target to be cooled with helium, as it becomes very hot due to the electron beams impinging. When cooled, the target reaches a temperature of approximately 900 °C.

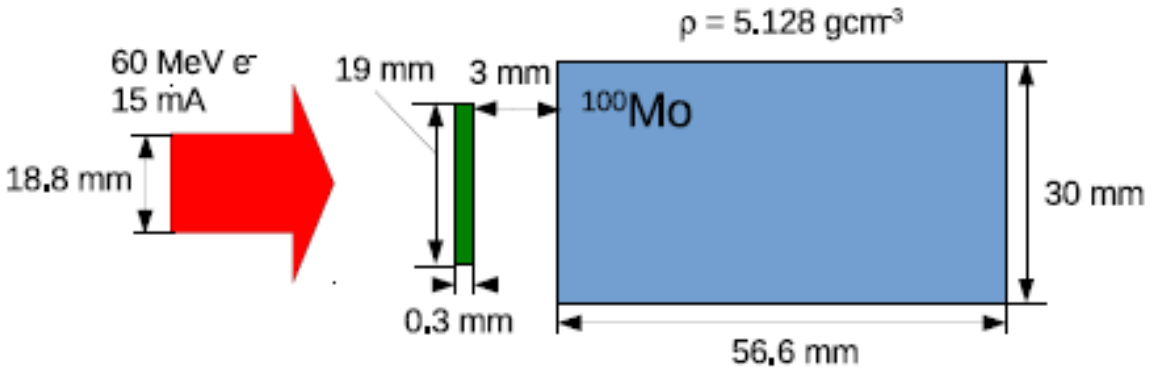

Figure 2.3: Geometry used in the research done by Bijers and Brandenburg [2].

The spectra calculated are shown in figures 2.4 and 2.5. As can been easily seen, the photons are peaked in the forward direction with their energy spectra extending up to beam energy. The neutrons show very different spectra; due to the fact that the neutrons are generated by giant-dipole resonance mechanism [2] they have an isotropic emission for neutrons with an energy below 10 MeV. Neutrons with a higher energy show a more anisotropic emission with energies also extending up to beam energy. Because in the real setup the target is irradiated with two electron beams the same spectra have to be added on top of the first spectra but with a 180° dimension shift. This has no effect on the neutron spectra, as the neutron emission is isotropic, but for the photon spectra it has a important effect. Because the photons are forward peaked there is now a region around the target, between 60° and 120°, that has a much lower photon flux compared to the rest of the area around the target. The reason why this is important will be discussed later. Per incident electron approximately $1.288 \cdot 10^{-2}$ neutrons are generated [2].

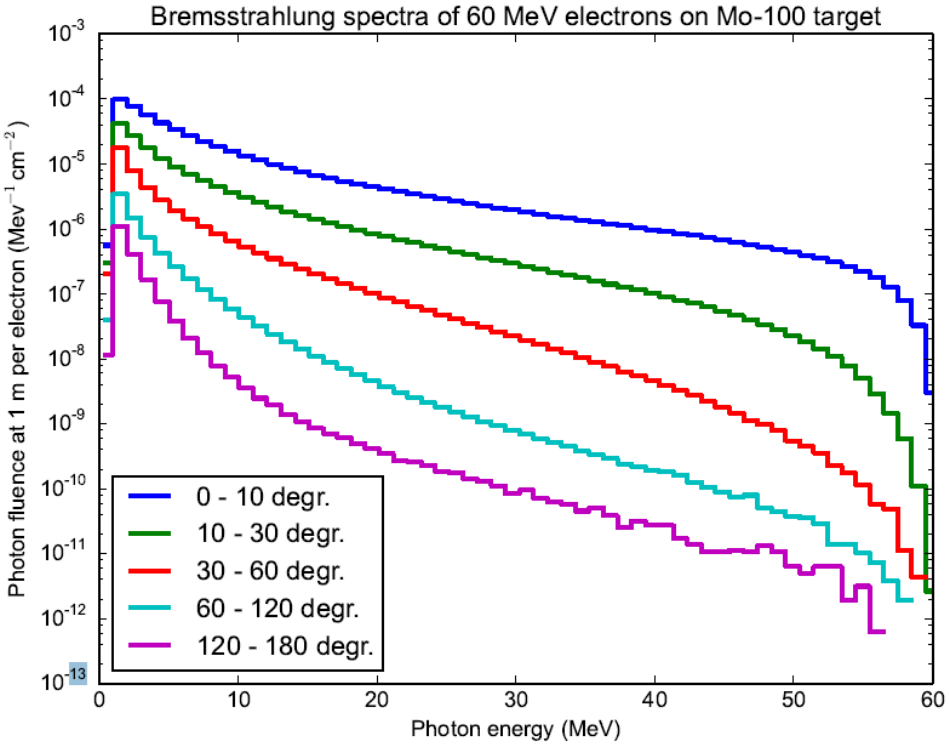

Figure 2.4: Left: Double-differential spectrum of the photons produced in the ^{100}Mo target [2].

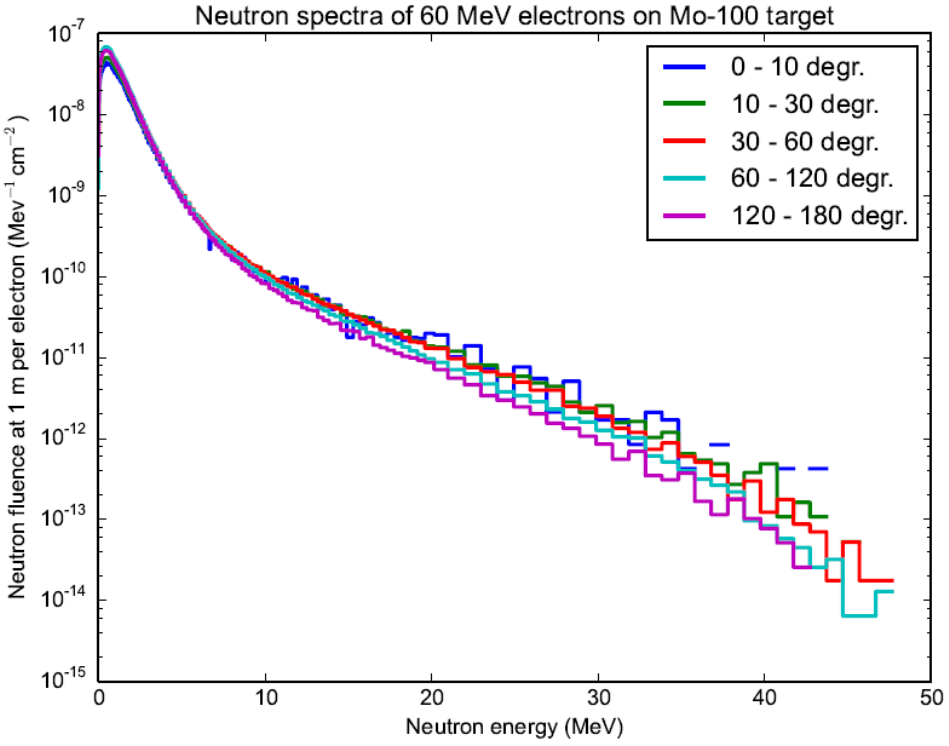

Figure 2.5: Left: Double-differential spectrum of the neutrons produced in the ^{100}Mo target [2].

2.2. Medical Isotopes

There are many different isotopes used for medical purposes. At the research location Petten alone 14 different isotopes are produced [16]. These isotopes are produced using two different methods: in the nuclear reactor or with a cyclotron. For this research project only the reactor isotopes are relevant. They are displayed in table 2.1.

Table 2.1: Isotopes produced at the research location Petten

Reactor isotopes	Cyclotron isotopes
molybdenum-99	indium-111
xenon-133	iodine-123
holmium-166	thallium-201
lutetium-177	rubidium-82
iodine-125 and 131	gallium-67
iridium-192	
strontium-89	
yttrium-90	

Of these isotopes a selection was made to be researched in this thesis. The isotopes chosen are holmium-166 and lutetium-177. ^{166}Ho was chosen because because this isotope was already being studied in the nuclear reactor of Delft. ^{177}Lu was chosen because it has a relatively high (n,γ) cross-section as can be seen in figure 2.6. Cross-sections will be discussed in section 2.3.1.

2.2.1. Holmium-166

^{166}Ho is an isotope that can be used for treating liver cancer. The most common form of liver cancer is hepatocellular carcinoma (HCC) [20]. Due to the fact that the only potential curative treatment is not a option for most people who suffer from this form, HCC is the 3rd cause of cancer related death. Therefore, alternative treatment methods for HCC are needed. A method that is currently being developed is intra-arterial microbrachytherapy. Brachytherapy [16] is a form of cancer treatment that places radioactive particles near or in a tumor. For HCC (and other types of liver cancer) these radioactive particles can be holmium-166 loaded poly(L-lactic acid) microspheres (^{166}Ho-PLLA-MS). The isotopes are passively targeted mainly to the tumor, limiting damage to healthy liver tissue. This is possible because the tumor receives blood from a different artery than the normal liver. The reason these microspheres are used is to make sure the radioactive holmium particles as close to the tumor as possible and stay there. Because of the size of the microspheres they lodge themselves in the tiny arteries surrounding the tumor.

^{165}Ho loaded PPLA-MS are produced by dissolving holmium acetylacetonate (HoAcAc) and PLLA in chloroform [20]. After that the solution is emulsified in a polyvinyl alcohol solution. When this solvent evaporates microspheres are formed.

Before ^{166}Ho yttrium-99 was used. ^{90}Y is a pure beta emitter, while ^{166}Ho is a combined beta-gamma emitter and highly paramagnetic. This means that besides irradiating the tumor the Ho loaded microspheres can also be used for creating images of the tumor and surrounding tissue, using either SPECT or MRI. The production equation of ^{166}Ho using neutron activation in a n,γ reaction:

$$^{165}_{67}\text{Ho} + \text{n} \rightarrow ^{166}_{67}\text{ Ho} + \gamma \tag{2.1}$$

^{166}Ho has a half-life of 26.8 hours and decays to the stable isotope erbium-166 through β^- decay:

$$^{166}_{67}\text{Ho} \rightarrow ^{166}_{68}\text{ Er} + \text{e}^- + \bar{\nu} + \gamma \tag{2.2}$$

The PLLA-MS do have a major flaw; there are made of organic molecules and are irreversibly damaged when their temperature becomes too high, rendering them useless. This increase in temperature is caused by energy deposition due to absorption of neutrons and photons. The

effect of this absorption on the integrity of the MS is researched in the nuclear reactor of the Delft University of Technology [20]. Results show that the structural integrity is maintained up to 7 h of neutron activation. Furthermore, calculations using the Monte Carlo method-based code MCNP5 [18] show that 93% of the total energy deposition came from the photons. This is why the region with low photon flux mentioned in section 2.1.2 is so important. In order for ^{166}Ho to be used as a medical isotope it has a required specific activity (SA) of 4.4-7.4 Ci·g^{-1} or $1.6 \cdot 10^2$-$2.7 \cdot 10^2$ GBq· g^{-1}. It is quite possible that the activation time in the lighthouse is significantly longer than in the reactor in Delft and that in order to maintain the structural integrity of the MS they have to be placed in the low photon-flux zone. But even if this is not necessary, placing the MS in this zone would yield higher quality MS, as the damage resulting of photon absorption is minimized.

2.2.2. Lutetium-177

^{177}Lu is a medical isotope of which a major application is neuroendocrine tumors. These are tumors where cellular receptors over-expressed on the surface of the cancer cells. Unlike ^{166}Ho MS ^{176}Lu is first irradiated with neutrons until the required SA of $19 \cdot 10^3$ Ci·g^{-1} or 700 TBq·g^{-1} is achieved, after which it is bonded to a molecule that targets the diseased area after injection. Because the bonding happens after irradiation ^{177}Lu does not suffer from negative effects of being irradiated with photons and in theory can be placed anywhere around or even in the ^{100}Mo core. ^{177}Lu is produced by neutron activation of ^{176}Lu in a n,γ reaction:

$$^{176}_{71}\mathrm{Lu} + \mathrm{n} \rightarrow ^{177}_{71}\mathrm{Lu} + \gamma \tag{2.3}$$

^{177}Lu has a half-life of 6.6 days and decays to the stable isotope hafnium-177 through β^- decay:

$$^{177}_{71}\mathrm{Lu} \rightarrow ^{177}_{72}\mathrm{Hf} + \mathrm{e}^- + \bar{\nu} + \gamma \tag{2.4}$$

2.3. Neutron activation

In order to maximize the efficiency of the Lighthouse the neutron absorption in the isotope targets placed around the ^{100}Mo has to be as high as possible. There are multiple parameters that influence this absorption.

2.3.1. Cross-section

The microscopic cross-section of an isotope, σ, quantifies the probability of the occurrence of a nuclear reaction. Each isotope has a certain cross-section for each nuclear reaction possible for that isotope. For the production of ^{166}Ho and ^{177}Lu the (n,γ) cross-section is the most relevant. The cross-section can be interpreted as a virtual surface associated with a certain isotope, perpendicular to an incoming particle, such that if the particle crosses the surface σ the reaction related to that cross-section occurs, and if the particle misses nothing happens. A more detailed explanation of the cross-section can be read in chapter 3.2 of *Energy from nuclear fission: an Introduction* [7]. A convenient unit for nuclear and particle collisions is the barn (symbol b), equal to 10^{-24} cm^2. The microscopic cross-section does not take into account that unless the material is very thin, the nuclei deeper in the material are shielded from the incoming neutrons by the nuclei near the surface. In order to correct for this a new symbol is introduced: Σ. This is referred to as the macroscopic cross-section. Its derivation can be read in chapter 2 of *Nuclear reactor analysis* [8]. Σ is defined as the product of the atomic number density A_d and the microscopic cross-section σ:

$$\Sigma = A_d \cdot \sigma \tag{2.5}$$

The macroscopic cross-section characterizes the the probability of neutron interaction in the a material of a certain volume. Because the dimension of Σ is inverse length it is not really a cross-section and it is more accurate to define it as the probability that a neutron reacts with a nucleus in a material after traveling a certain distance. Using this definition the probability that a neutron has its first reaction between x and x+dx can be written as:

$$p(x)dx = \Sigma \mathrm{e}^{-\Sigma x} dx \tag{2.6}$$

If ν is the neutron speed than the product of ν and Σ can be defined as the interaction frequency:

$$\nu \cdot \Sigma = \text{interaction frequency} \tag{2.7}$$

By multiplying the interaction frequency with the neutron density N_N the reaction-rate density F can be calculated:

$$F = \nu \cdot \Sigma \cdot N_n \tag{2.8}$$

Because the product of the neutron speed and the neutron density is used very often it was given its own name; the neutron flux ϕ. This gives rise to the final equation for the reaction-rate density:

$$F = \Sigma \cdot \phi \tag{2.9}$$

which has units $cm^{-3} \cdot s^{-1}$. By integrating over the volume the number of neutrons absorbed in the target can be found.

2.3.2. Thermal neutrons

The cross-section for a nuclear reaction is not a constant, but often depends on the energy of the incoming particle. In figure 2.6 the dependence of the (n,γ) cross-sections of five isotopes on the energy of incoming neutrons can be seen. It is easy to see that the cross-sections are

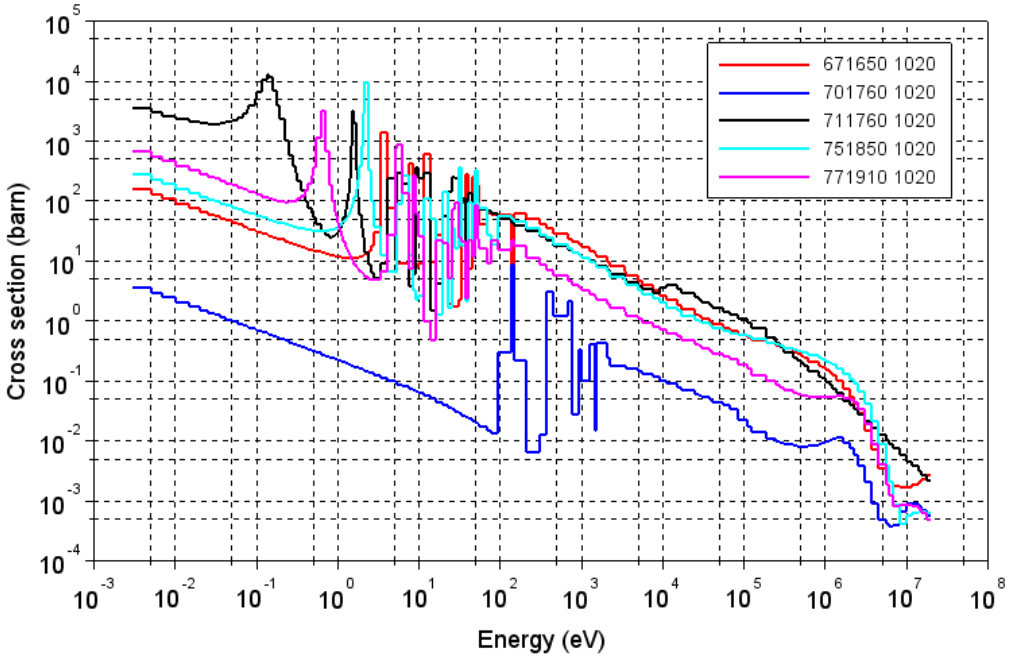

Figure 2.6: The (n,γ) cross-sections for ^{165}Ho (red), ^{176}Yb (blue), ^{176}Lu (black), ^{185}Re (cyan) and ^{191}Ir (purple). Data supplied by the NEA [10]

highest for neutrons with a low energy. These neutrons are called thermal neutrons and have an energy of around 0.025 eV. As described earlier, the neutrons emitted from the molybdenum target have an energy extending up to 60 MeV. This means they have to be slowed down in order to increase the absorption of the neutrons in the target isotopes. In nuclear reactors this is done using moderators.

In a moderator, neutrons transfer their kinetic energy to the nuclei of the substance the moderator is made of through series of elastic collisions. This transfer is more efficient if the mass of the nucleus is comparable to that of the neutron while if the mass of the nucleus if much greater than that of the neutron the transfer becomes very inefficient. The the average

logarithmic energy loss per collision is defined as ξ or the lethargy gain [8]. The dependency of ξ on the mass A of a nucleus a neutron collides with is given by the following equation:

$$\xi = 1 - \frac{(A-1)^2}{2A} \cdot \ln\left(\frac{A+1}{A-1}\right) \tag{2.10}$$

Besides nucleus mass the scattering cross-section of the material is also important. Nuclei with a high scattering cross-section Σ_s have a bigger chance of scattering a neutron and slowing it down. The product of the lethargy gain and the scattering cross-section is defined as follows:

$$\text{Moderating power} \equiv \xi \cdot \Sigma_s \tag{2.11}$$

Finally, it is also very important that the moderator material is a weak absorber of neutrons, which means its absorption cross-section, Σ_a, has to be low. By dividing the moderating power with the absorption cross-section the moderating ratio can be defined:

$$\text{Moderating ratio} \equiv \frac{\xi \cdot \Sigma_s}{\Sigma_a} \tag{2.12}$$

For a material to be a good moderator is has to have a high moderating power. In table 2.2 the parameters of some standard moderators are displayed.

Table 2.2: Slowing down parameters of standard moderators [8]

Moderator	A	ξ	ρ [g/cm^3]	Number of collisions from 2 MeV to 1 eV	$\xi\Sigma_s$	$\xi\Sigma_s/\Sigma_a$
H_2O	-	0.920	1.0	16	1.35	71
D_2O	-	0.509	1.1	29	0.176	5670
He	4	0.425	gas	34	$1.6 \cdot 10^{-5}$	83
Be	9	0.209	1.85	69	0.158	143
C	12	0.158	1.60	91	0.060	193
^{238}U	238	0.008	19.1	1730	0.003	0.0092

From table 2.2 it is clear that heavy water is a very good moderator, but because of the high temperature of the molybdenum target it can not be used in this setup. Two other candidates are beryllium and graphite. Both of these materials are often used in nuclear reactors. The moderating ratio of graphite is higher than that of beryllium, indicating that it would be a better moderator. Beryllium, however, has an attribute that might make it more useful than graphite. It has a relatively high (n,2n) cross-section, which means it can be used to increase the neutron flux originating form the molybdenum target.

It is possible that a neutron leaves the moderator without having lost enough energy to be absorbed in the target and passes through it. In order to try to have this neutron still be absorbed in the target a reflector could be placed behind the target. In a nuclear reactor a reflector surrounds the core of the reactor in order to reflect neutrons directed towards the exterior, decreasing neutron leakage. These reflectors are often made of the same materials as moderators. By placing a reflector behind the target neutrons passing through the target could be slowed down and reflected to the target, boosting absorption in the target isotopes.

2.4. Isotope production

During the irradiation of the target nuclei the atoms that already have been made radioactive will start to decay. Starting with a number N_r radioactive atoms the decay can be described with the following equation:

$$dN_r = -\lambda N_r dt \tag{2.13}$$

The solution of this equation is:

$$N_r(t) = N_{r,0} \mathrm{e}^{-\lambda t} \tag{2.14}$$

where N_r is the number of remaining radioactive atoms at time t, λ the decay constant of the radioactive isotope in question and $N_{r,0}$ the number of radioactive atoms at $t = 0$.

But because there are also new radioactive atoms being produced equation 2.13 has to be modified with a factor that symbolizes the production of the radioactive atoms. Introducing χ as the number of neutrons absorbed in the target per second (and thus the number of radioactive atoms produced per second), equation 2.13 becomes:

$$dN_r = (\chi - \lambda N_r)dt \tag{2.15}$$

which has the solution:

$$N_r(t) = \frac{\chi}{\lambda}(1 - \mathrm{e}^{-\lambda t}) \tag{2.16}$$

In order for this equation to be correct the assumption has to be made that the absorption rate in the target remains constant during the irradiation time. If this project is to be considered feasible the required specific activity has to achieved within 2.5 to 3 times the half-time of the produced isotope, which is considered the irradiation time limit.

2.5. Gamma shielding

In order to protect the holmium loaded microspheres and to decrease the effect of the photons the moderator can be replaced with a gamma shield. Materials with high densities are great photon absorbers. A material that is often used as a gamma shield is lead, but because of its low melting point it is not usable in this setup. Another great gamma shield material is tungsten. It has a very high density and because of its high melting point (3410 °C) [5] it can be used in high temperature environments. The downsides of tungsten are that it is very expansive and difficult to fabricate. This means it is usually used for small shields near the gamma source.

The gamma attenuation factor A_f is described by the following equation [5]:

$$A_f = B \cdot \mathrm{e}^{-\mu \cdot x/\cos\theta} \tag{2.17}$$

where B is the buildup factor, μ the linear attenuation coefficient, x the shield thickness and θ the angle between the normal of the shield and the incoming radiation. The buildup factor is the ratio of the total amount of photons and photons that experienced no collisions.

3

Geometries

In this thesis two types of geometries were tested. The first geometry was a spherical molybdenum core with the same volume as the molybdenum core used in the research done by H. Beijers and S. Brandenburg [2] surrounded by multiple spherical layers consisting of different materials. This geometry does not closely resemble the real-life setup or the setup used in the simulations run by Bijers and Brandenburg [2]. Nevertheless, this is a good starting point, as it is easier to create in Serpent and needs less time to complete the simulation as it is a simpler geometry. Furthermore, the simpler geometry made it easier to understand how Serpent [12] handles its input and to understand the meaning of its output, as the manual was fairly lacking in this regard.

The second geometry resembled the real setup more closely. It consists of a cylindrical molybdenum core, again with the same volume as in the simulations of done by Beijers and Brandenburg. Around this cylinder multiple cylindrical layers were placed. Although this is still different from the real setup, it is a much better approximation than the spherical geometry.

3.1. Target volume

It was decided to have the target volume remain constant throughout the simulations, in order to make it easier to see the influence of certain parameters. For both ^{165}Ho and ^{176}Lu the mass that was to be irradiated was set to 20 g. This mass was chosen for holmium because one of the goals was to be able to reach the required specific activity for 10-20 g holmium. The mass of lutetium was decided to be the same as that of holmium to make comparison easier. For lutetium the target volume was easy to calculate, simply its mass divided by its density. The temperature of the lutetium was set to 1200 K, the reason for which will be explained in the next chapter. Using linear interpolation the density of Lu was calculated at this temperature. This method differs from the real temperature dependence of the density of Lu, but the effects of this approximation were considered negligible in the scope of this research project. Using this method, the lutetium target volume was calculated to be approximately 2.1 cm^3.

This is not as simple for the holmium target, due to the fact that the holmium is loaded into microspheres. In order to calculate the volume of the holmium target the following data has to be known: the volume of a single microsphere, the mass of a single microsphere and the mass percentage of holmium in a microsphere. According to information provided by ASML there is 110 mg holmium in 600 mg microspheres [6]. Furthermore, the mean diameter of the microspheres is around 30 µm and 700 mg microspheres consists of approximately 33 million spheres [20]. When put in a container the spheres do not fill the space perfectly, so it is assumed that they have a 50% filling rate. Combining all this information gives a holmium target volume of approximately 145 cm^3. The 2D figures displayed in the following sections were generated by Serpent. In all figures the z-axis is aligned vertically, with the x- or y-axis

being aligned horizontally. The electron beams impinge on the target along the positive and negative y-axis. The 3D figures were created using Rhinoceros [15].

3.2. Spherical geometry

In figure 3.1 the cross section of the spherical geometry in the yz-plane at x=0 can be seen. Starting in the middle, the red circle is the ^{100}Mo target. The first green layer around the core is the moderator. Next is the black circle, which is the holmium or lutetium target. Because the target volume is so small compared to the rest of the geometry it is drawn as a thin line. The large green layer outside of the target is the reflector, while the blue layer is made of boron that absorbs all neutrons leaving the reflector. The reason for this layer will be explained in the next chapter. The black areas are defined as 'outside' of the geometry, which means that neutrons that enter these areas are terminated.

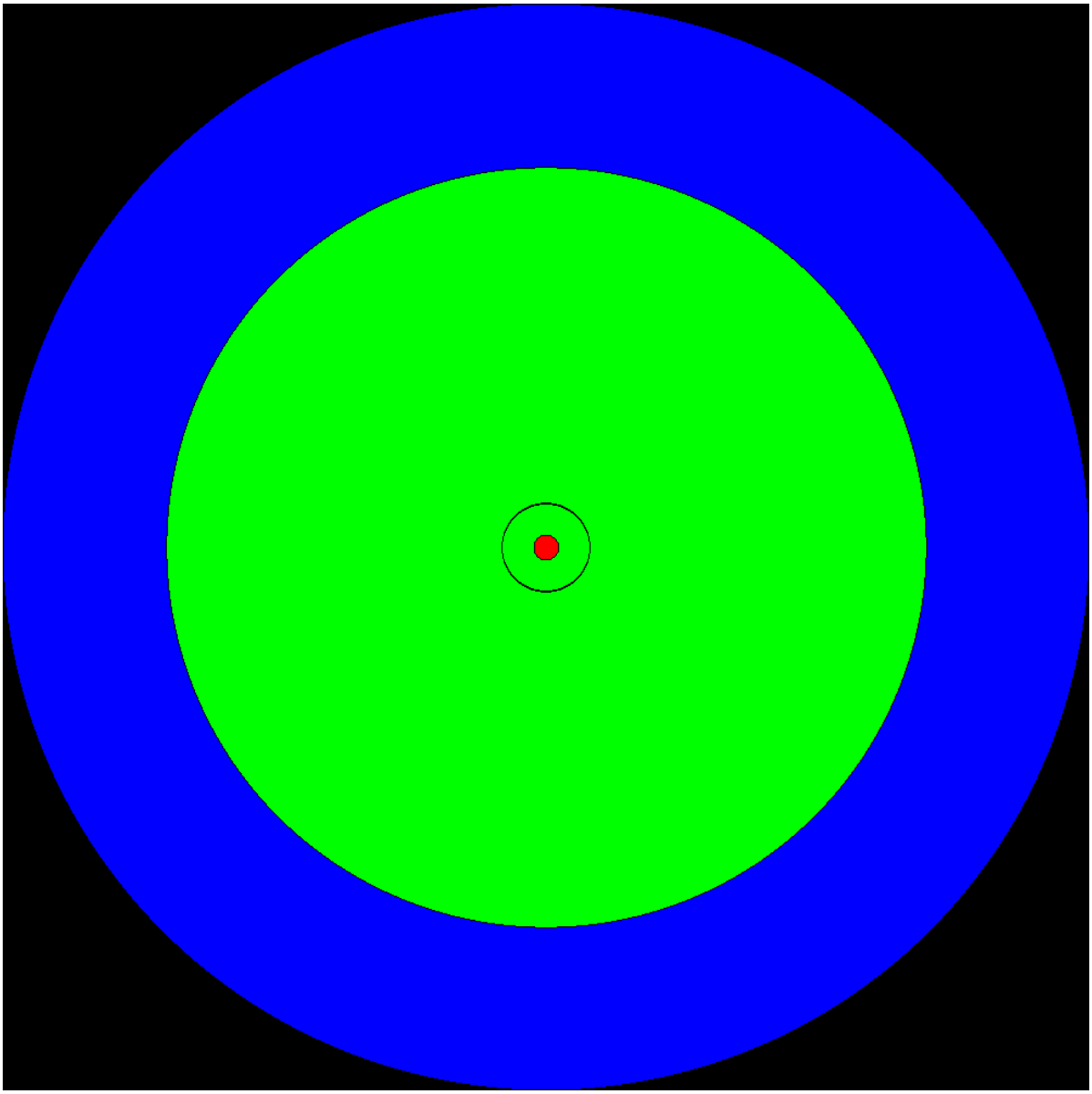

Figure 3.1: Cross section of the spherical geometry in the yz-plane at x=0. The z-axis is aligned vertically and the y-axis horizontally. The red circle is the molybdenum target, the inner and outer green circle are the moderator and reflector respectively, while the black line in between is the holmium or lutetium target. The blue ring is the boron absorption layer. The radius of the outer surface of the boron layer is around 70 cm.

In order to have a better idea of how the geometry is constructed a modified version of the geometry can be seen in figure 3.2. The layers now all have more or less the same thickness, which makes it much easier to understand what the variables R_1 to R_5 represent. Again, the red circle is the molybdenum target, the first green circle the moderator, the purple circle the holmium or lutetium target, the second green circle the reflector and the blue circle the boron absorption layer.

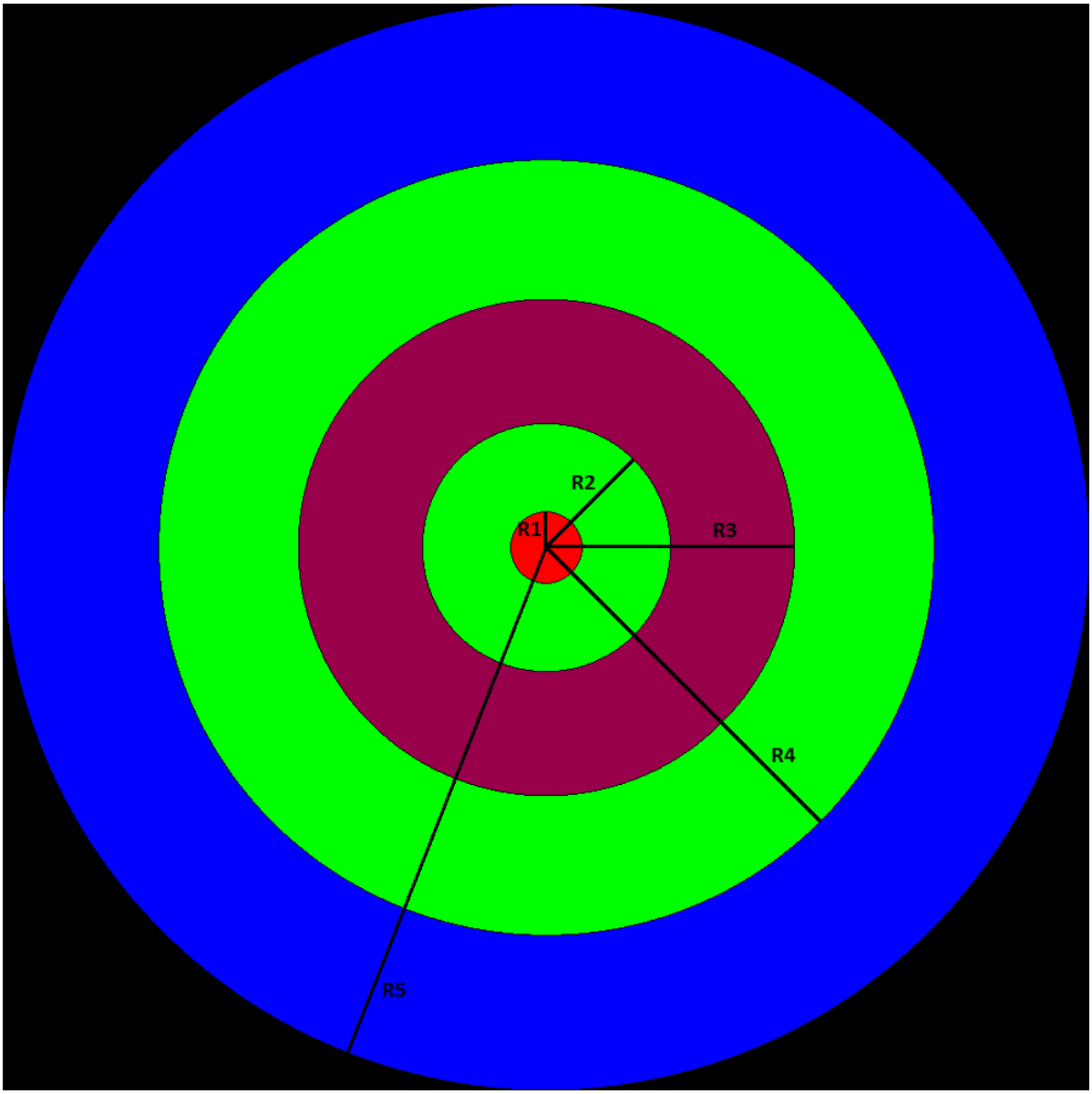

Figure 3.2: Cross section of the spherical geometry in the yz-plane at x=0. The thickness of the layers has been modified to get a more clear overview. All colors represent the same materials as in figure 3.1, while purple now represents the holmium or lutetium target.

The radius R_1 of the core is constant at approximately 2.3 cm, as this radius gives to core the same volume as the core used to determine the neutron and gamma spectra [2], around 51 cm^3. R_2 can be chosen at random, except that it has to be larger than R_1, which is fairly self-explanatory. R_3 is dependent on R_2, as the volume of the target has to remain constant. This means that R_3 is given by:

$$R_3 = \left(\frac{3}{4\pi} \cdot V + {R_2}^3\right)^{1/3} \tag{3.1}$$

where V is the volume of the target. R_4 again can be choses at random, as longs as it is larger than R_3 and the same goes for R_5. By varying these numbers it should be possible to find the maximum neutron absorption in the target.

In figure 3.3 a 3D visualization of the spherical geometry can be seen. The boron absorption layer is omitted as it will not be a part of the real setup.

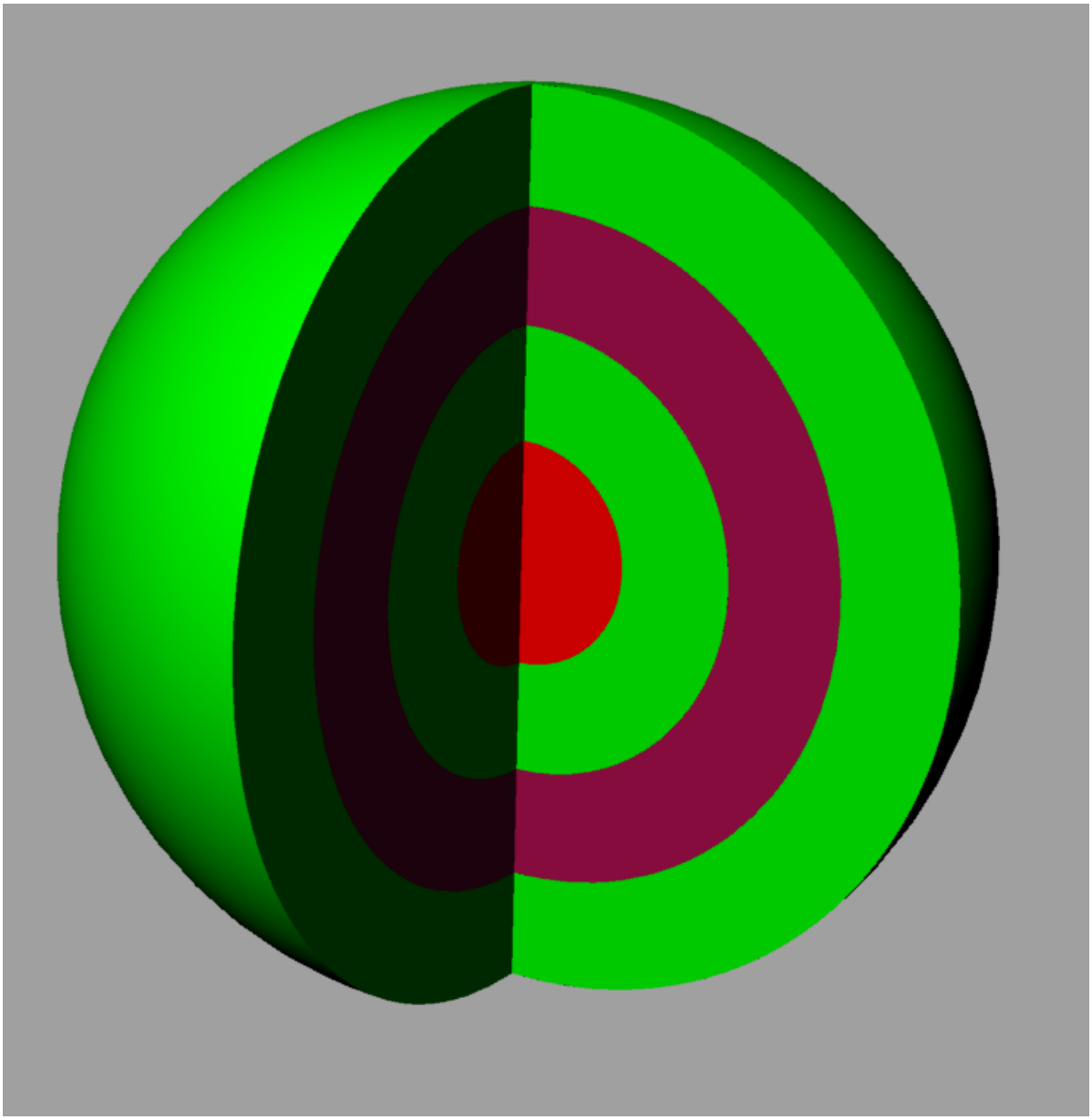

Figure 3.3: 3D visualization of the spherical geometry. The boron absorption layer is omitted.

3.3. Cylindrical geometry

In figures 3.4 and 3.5 two different cross sections of the cylindrical geometry can be seen. In figure 3.4 the cross section is in the yz-plane at x=0 or side view. In figure 3.5 the cross section is in the xz-plane at y=0 or front view. The red inner volume, in this case a cylinder, as the molybdenum core, with the green layer surrounding it the moderator. On top of that there are two black rings and a blue one. The black ones are defined as 'void', meaning the neutrons pass through these volumes without any interaction. The blue one is the target. The reason for the target to be flanked by these 'void' rings is to make sure the target is in the region with the lowest photon flux. The final green cylindrical layer is the reflector. The entire cylindrical setup is surrounded by a spherical boron absorption layer. The shape of this layer does not matter for the results, but using a sphere made the constructing of the geometry in Serpent easier than if a cylindrical shape was used.

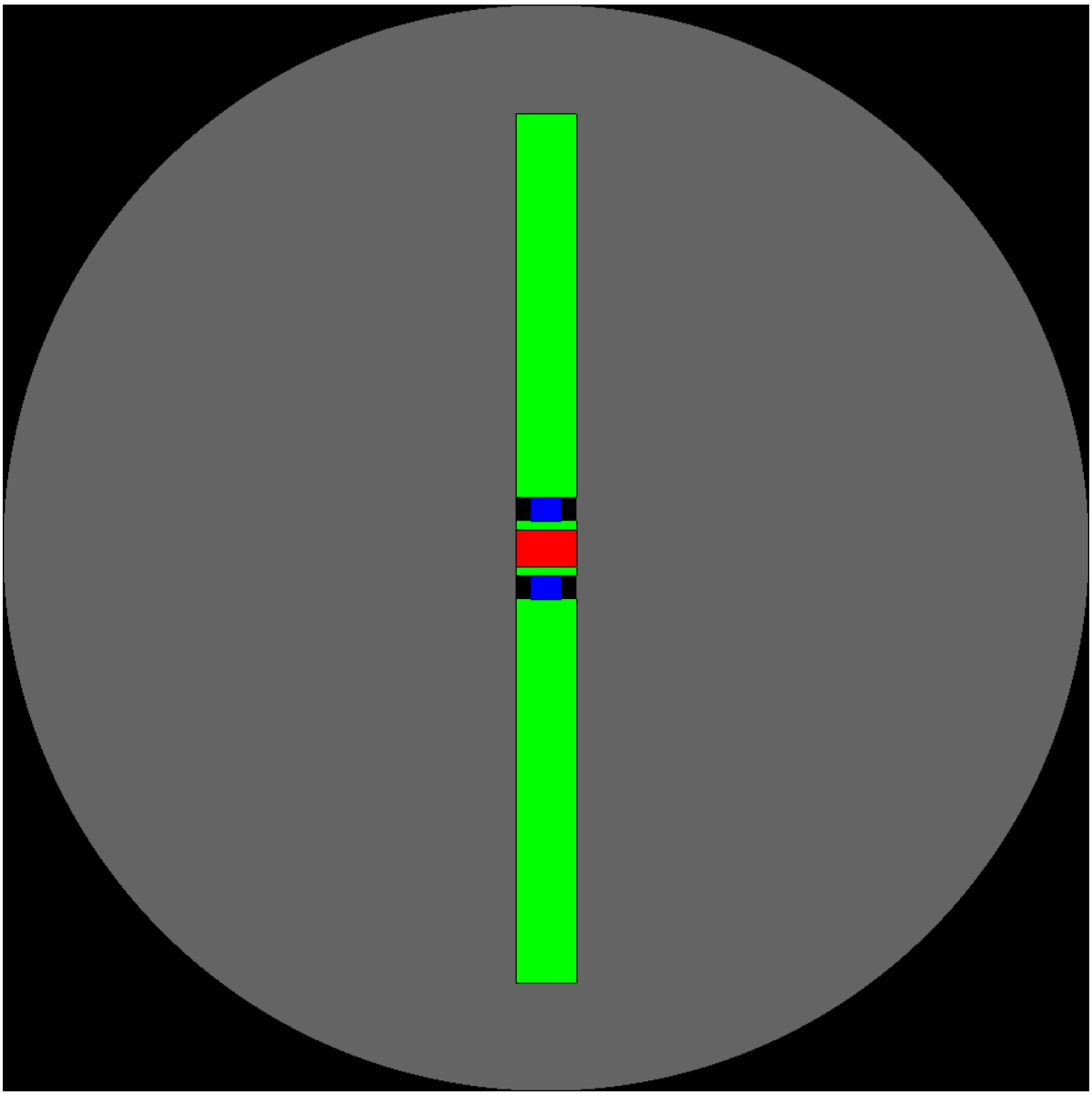

Figure 3.4: Cross section of the cylindrical geometry in the yz-plane at x=0. The y-axis is aligned horizontally, while the z-axis is aligned vertically. The red cylinder is the molybdenum target with the green layer surrounding it the moderator. The blue ring around the moderator is the holmium or the lutetium target, with the black parts being empty space. The outer green layer is the reflector. The grey sphere surrounding it all is the boron absorption layer. The radius of the reflector is 40 cm.

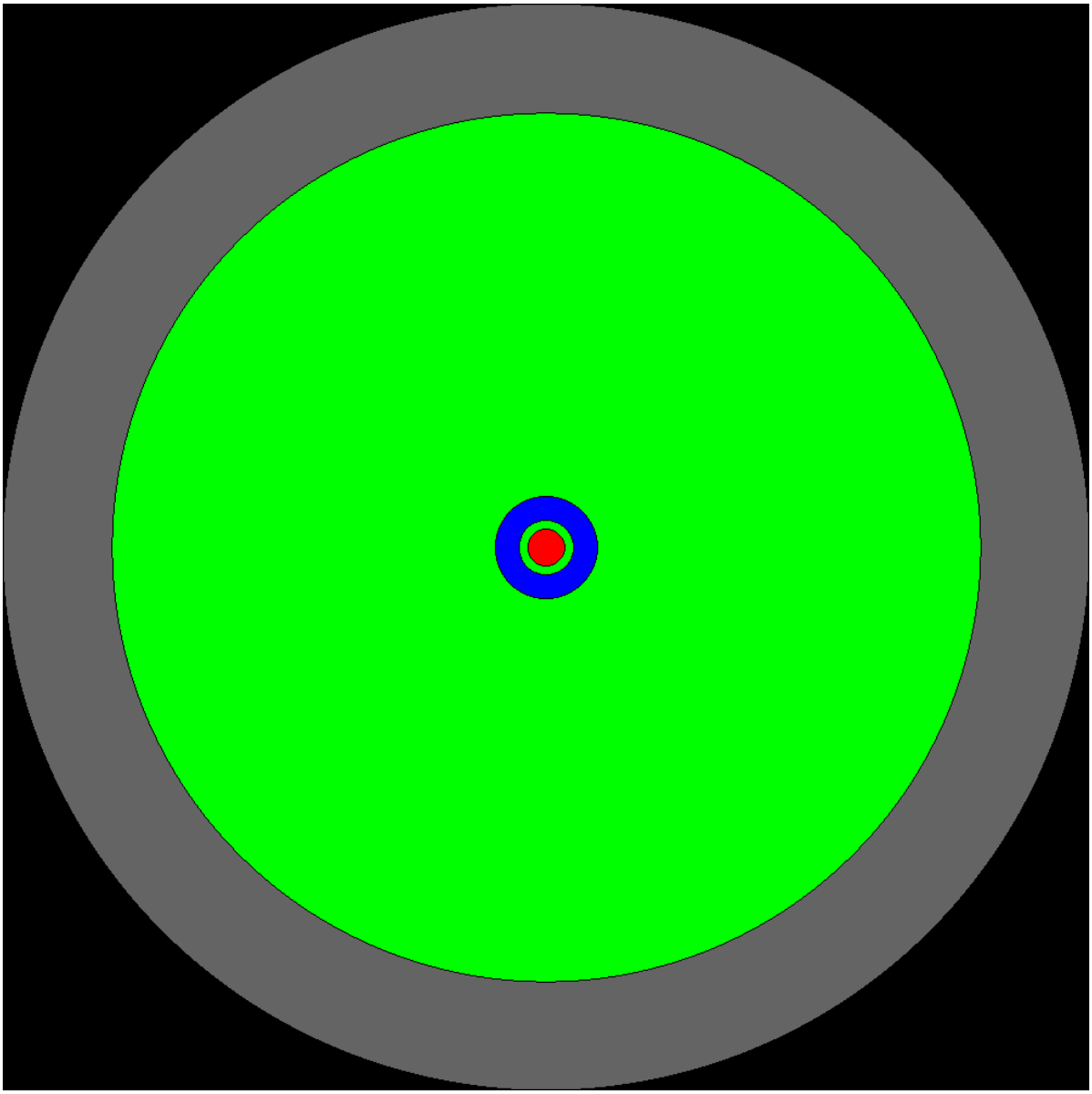

Figure 3.5: Cross section of the cylindrical geometry in the xz-plane at y=0. The x-plane is aligned horizontally, while the z-plane is aligned vertically. The colors represent the same materials as in figure 3.4

Modified versions of figures 3.4 and 3.5 can be seen in figures 3.6 and 3.7. Like the spherical geometry, this is done to get a better picture of how the cylindrical geometry is constructed. In this case R_1 to R_4 are the radii of the cylindrical shapes/shells, while R_5 is the radius of the spherical absorption layer. It was decided to keep the length of the cylindrical core the same as the length of the molybdenum block used in Groningen, which is 5.56 cm. This was done in order to have the molybdenum target to resemble the molybdenum target from Groningen as close as possible while still using a cylindrical shape. The black line in the middle of the core lies on the y-axis at x=0 and z=0. This meant that in order for the core to have the same volume, around 51 cm^3, R_1 had to be approximately 1.69 cm. R_2 can be chosen at will, as long as it is larger than R_1. R_3 is again dependent on R_2, as the target volume has to remain constant. R_3 is given by the following equation:

$$R_3 = (\frac{V}{W \cdot \pi} + R_2^2)^{1/2} \tag{3.2}$$

Where V is the volume of the target and W the width of the target in the y-direction. Just like

before, R_4 is free to choose, keeping in mind that it has to be larger than R_3 , and the only restriction on R_5 is that it has to be larger than R_4.

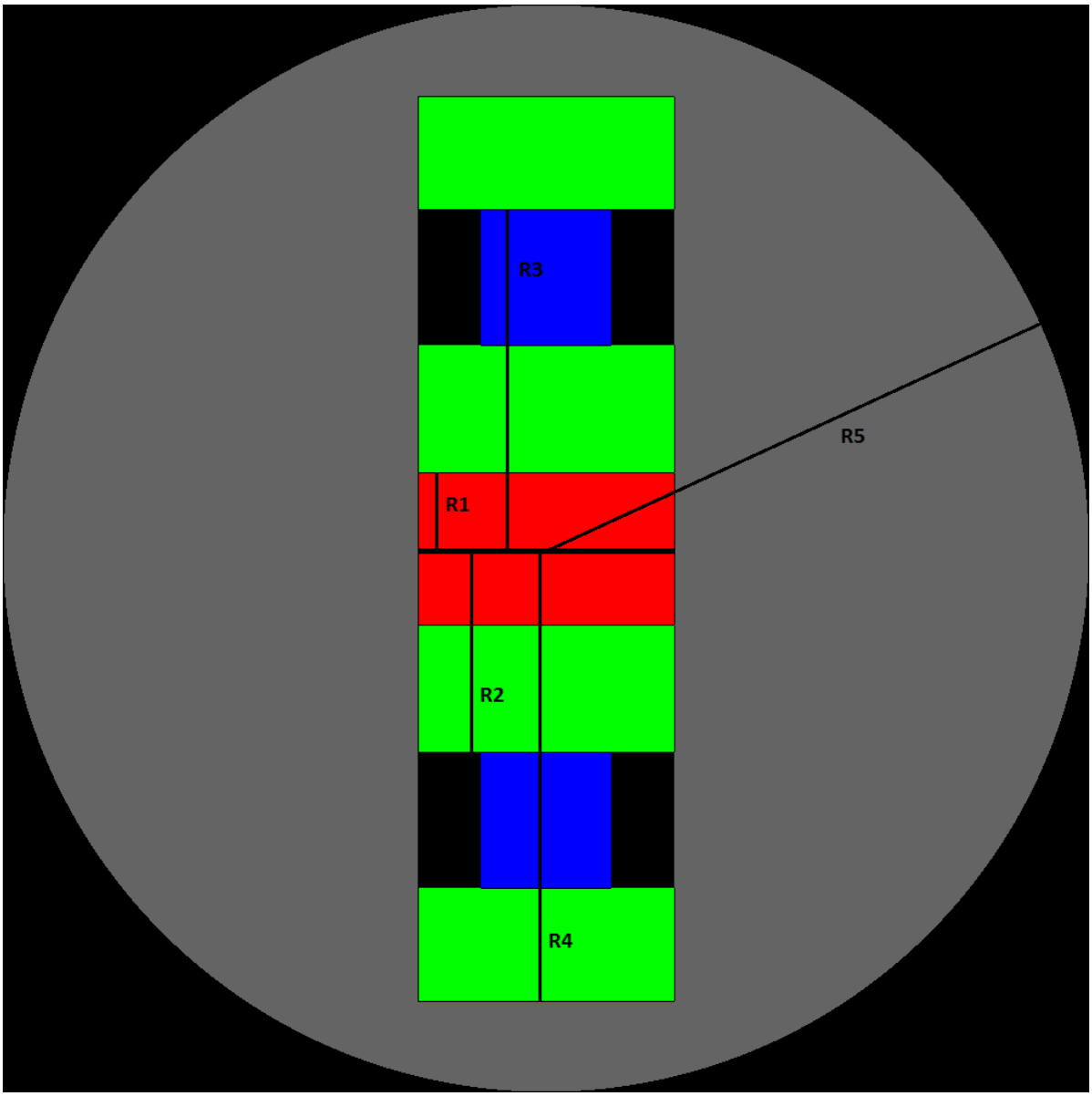

Figure 3.6: Cross section of the cylindrical geometry in the yz-plane at x=0. The thickness of the layers has been modified to get a clearer overview of the geometry. R_1 to R_4 are the radii of the cylindrical layers, while R_5 is the radius of the spherical absorption layer.

In figure 3.8 a 3D visualization of the cylindrical geometry can be seen. The boron absorption layer is again omitted.

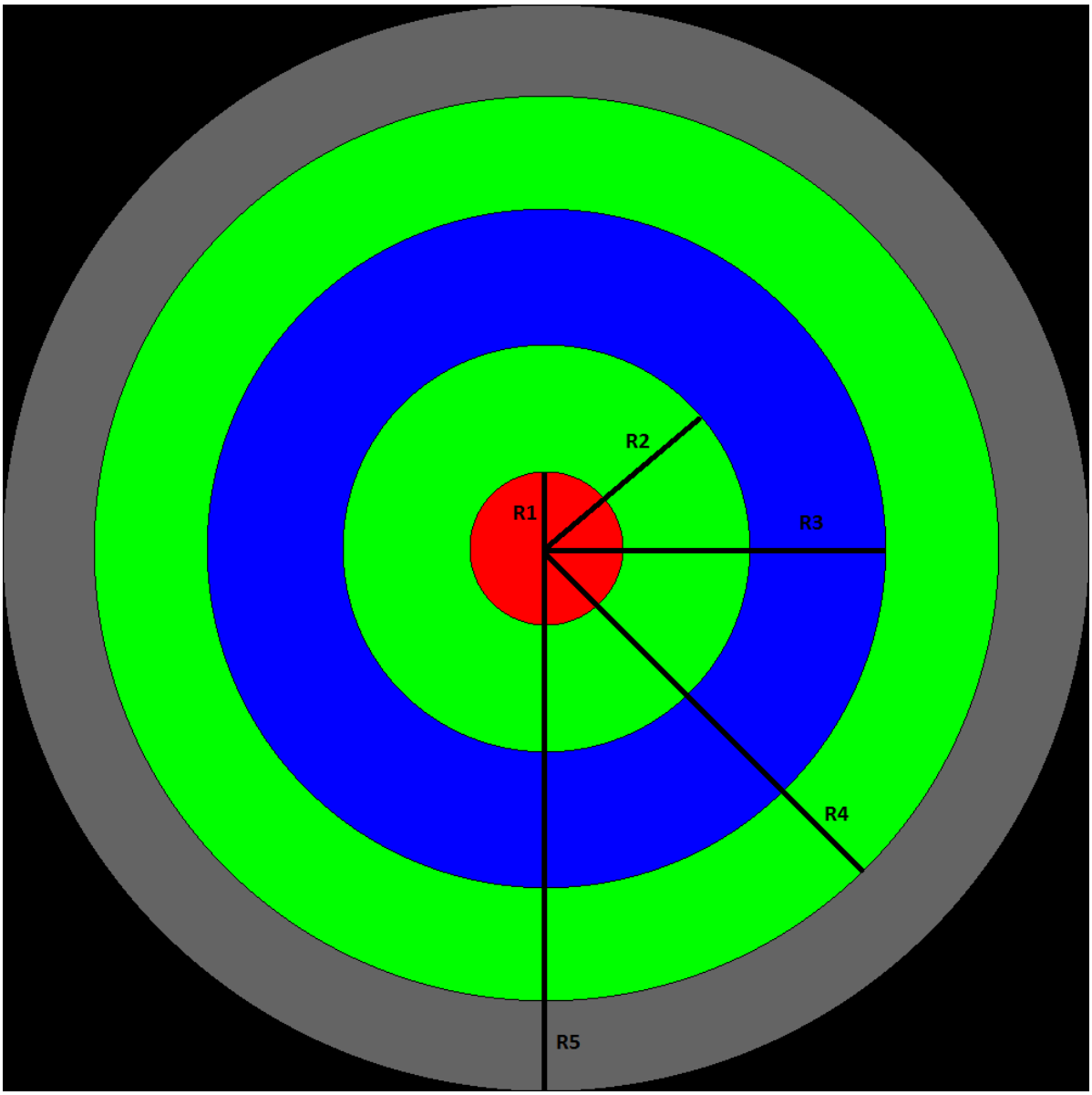

Figure 3.7: Cross section of the cylindrical geometry in the xz-plane at y=0. The thickness of the layers has been modified to get a clearer overview of the geometry. R_1 to R_4 are the radii of the cylindrical layers, while R_5 is the radius of the spherical absorption layer.

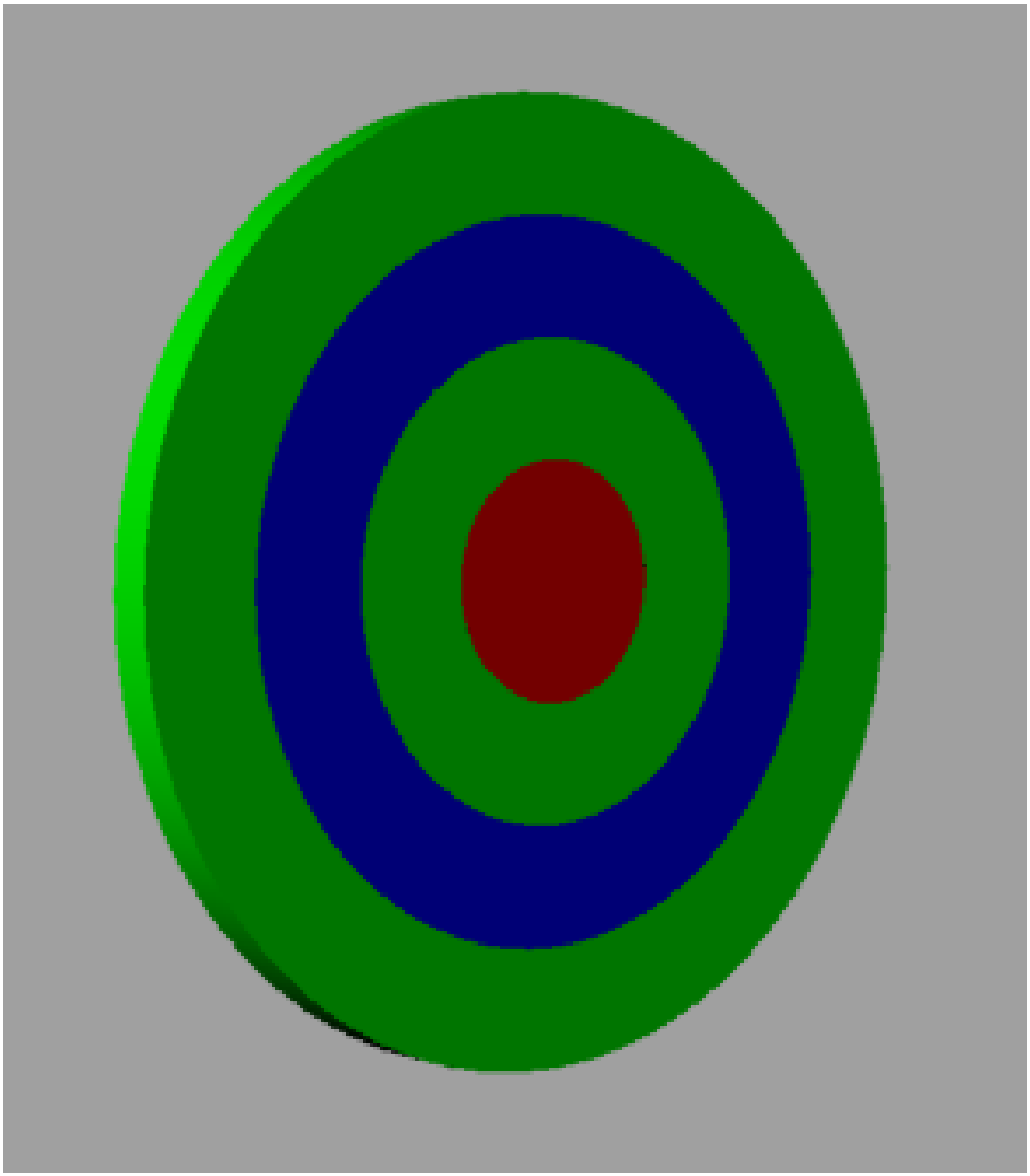

Figure 3.8: 3D visualization of the cylindrical geometry. The boron absorption layer is omitted.

3.3.1. Reflector panels

To increase neutron absorption in the target two reflector panels were placed in front and behind the setup, as can be seen in figure 3.9. Furthermore, the two void rings flanking the target are replaced with reflector material. The black tube extending in the negative and positive y-direction is 'void' and allows the electron beams to impinge on the molybdenum target without interacting with any material.

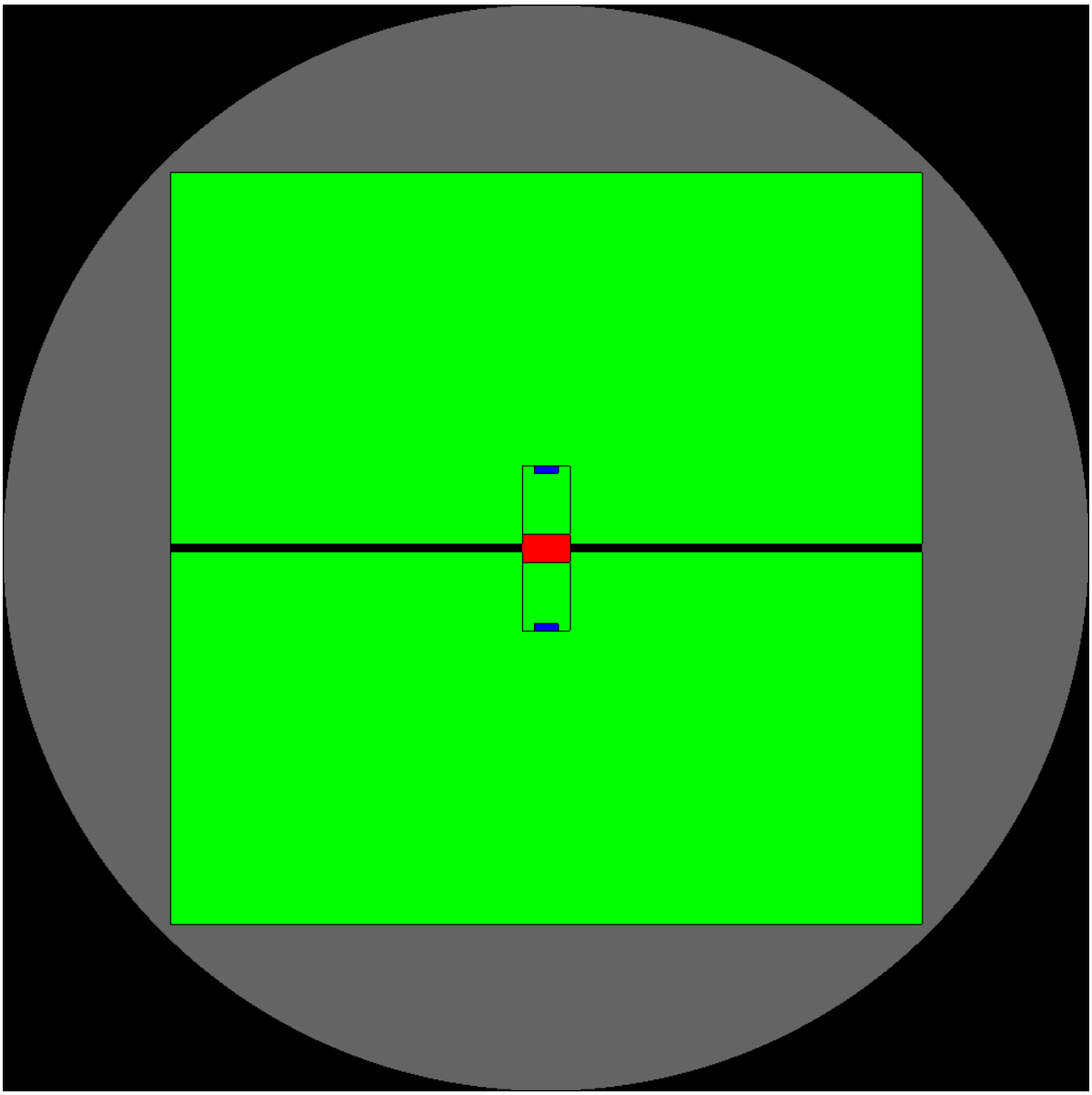

Figure 3.9: Cross section of the cylindrical geometry with extra reflector panels in the yz-plane at x=0. The radius from the y-axis of the total reflector is 40 cm and it extends 40 cm in the positive and negative y-direction from the xz-plane at y=0.

In figure 3.10 a 3D visualization of the cylindrical geometry with added reflector panels can be seen. The black circle is an empty tube through which the electron beam can enter.

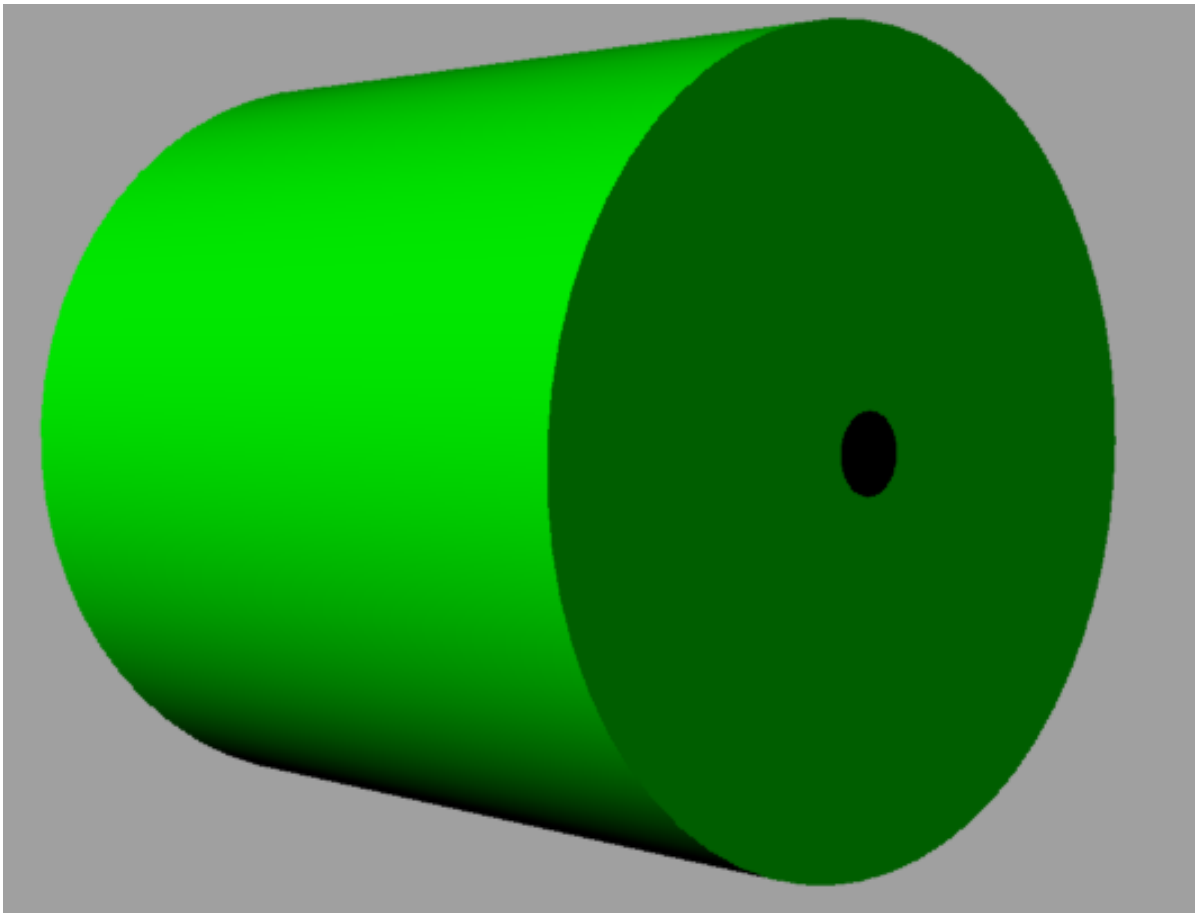

Figure 3.10: 3D visualization of the cylindrical geometry with added reflector panels. The boron absorption layer is omitted. The black circle is the entrance for the electron beam impinging from this side.

3.3.2. Tungsten gamma shield

In order to reduce the gamma flux through the holmium target the moderator was replaced with a gamma shield. This can be seen in figure 3.11, where the yellow layer is the shield. The standard material for a gamma-shield is lead, but because the high temperature of the core it can not be used here. Instead of lead, tungsten was chosen, as its melting point of 3410 ^{o}C [5] is much higher than the temperature of the molybdenum target and because it is a very heavy element, which is very efficient at stopping gamma radiation.

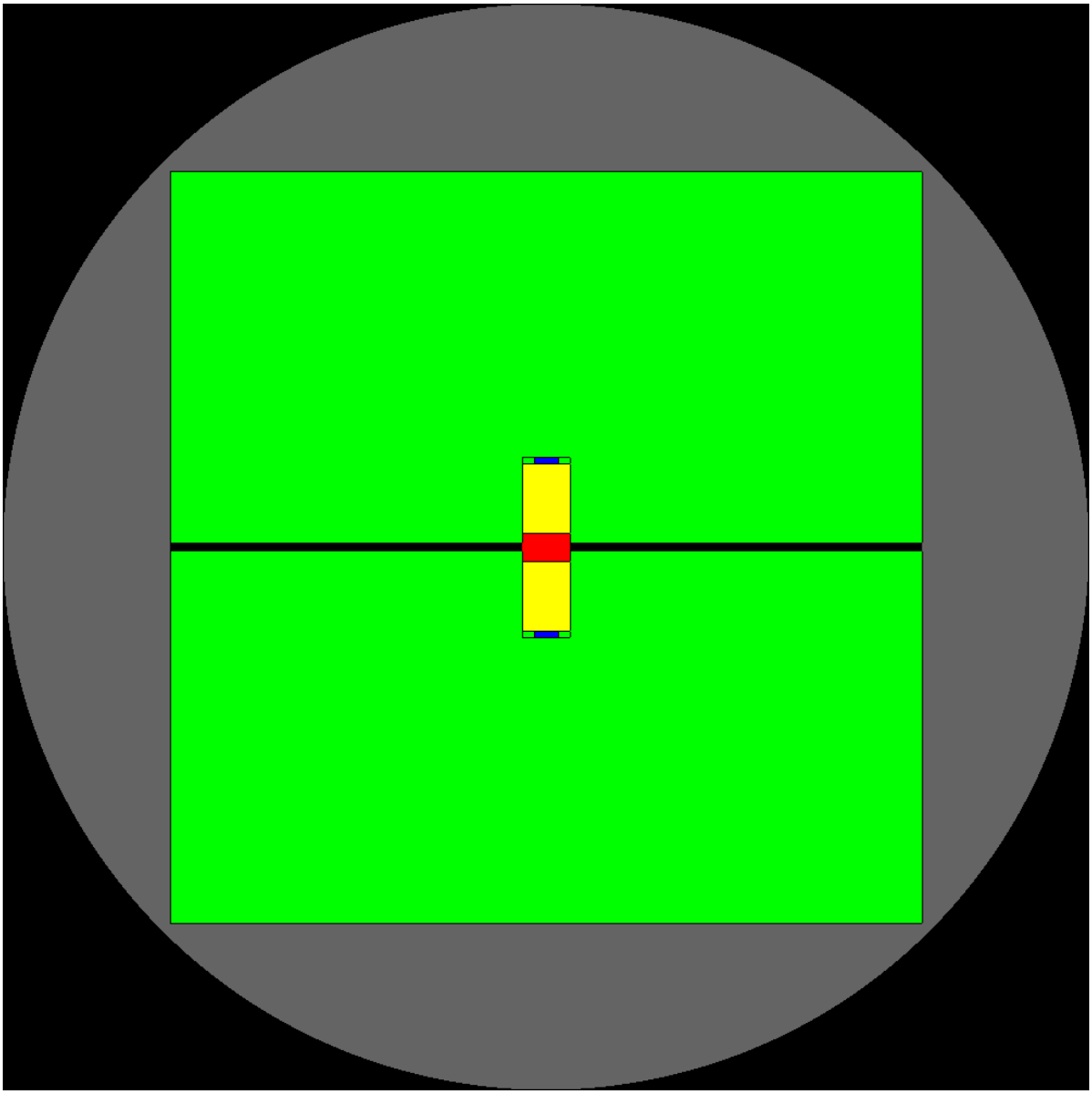

Figure 3.11: Cross section of the cylindrical geometry with added reflector panels with a tungsten gamma shield instead of a moderator, the shield being the yellow layer.

4

Computational Method

The neutron propagation and absorption was simulated using Serpent, which started out as a neutron reactor physics code, but now has many more applications.

4.1. Serpent

4.1.1. Serpent overview

Serpent is a multi-purpose three-dimensional continuous-energy Monte Carlo particle transport code [12]. Originally developed for modeling nuclear reactors the latest version of the code has many more applications which can be roughly divided into the following two categories:

1. Traditional reactor physics applications, including spatial homogenization, criticality calculations, fuel cycle studies, research reactor modeling, validation of deterministic transport codes, etc.

2. Neutron and photon transport simulations for radiation dose rate calculations, shielding, fusion research and medical physics

Of these applications the second one is the most important to this thesis, as neutron transport and absorption are the main subjects. A more detailed description of the main features and capabilities of Serpent can be read on the corresponding website:
http://montecarlo.vtt.fi/index.htm.

4.1.2. Monte Carlo method

The Monte Carlo method is a class of computational algorithms often used in physics. Its name was given because the method revolves around random selection of random events. A major benefit of the Monte Carlo method is that it can solve problems with few approximations, with the disadvantage that in order to get results with a very high accuracy many simulations are needed, which increases cpu time. The statistical uncertainty decreases with 1 over the square root of number of simulations run. Iván Lux and László Koblinger [13] use the following definition to describe the Monte Carlo method:

In all applications of the Monte Carlo Method a stochastic model is constructed in which the expected value of a certain random variable is equivalent to the value of a physical quantity to be determined. This expected value is then estimated by the average of several independent samples representing the random variable introduced above. For the construction of the series of independent samples, random numbers following the distributions of the variable to be estimated are used.

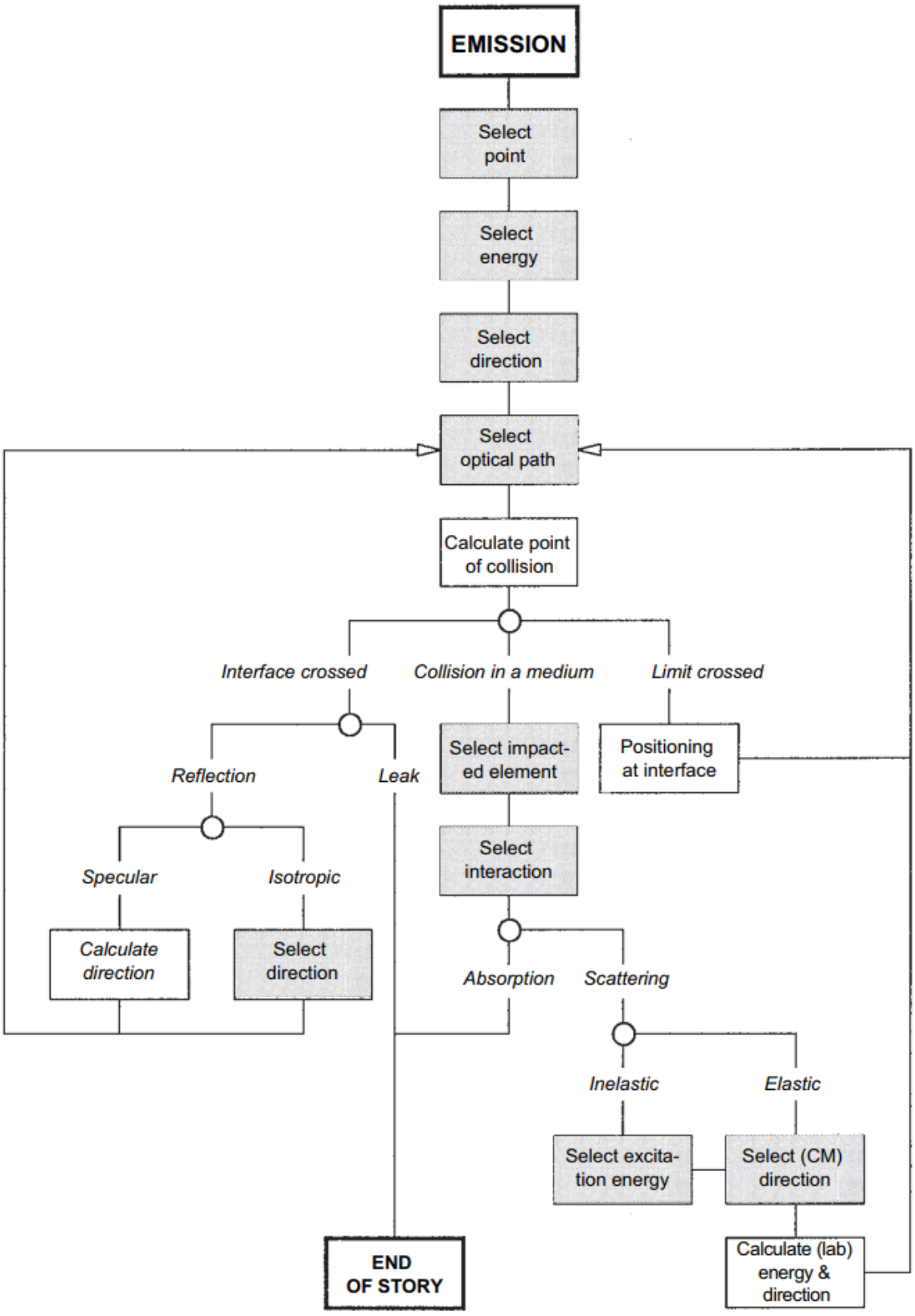

Figure 4.1: Simulation of the life story of a neutron using the Monte Carlo method [17].

Everything that happens to a neutron between its emission and absorption or leakage from

the system is a series of independent events. There are two types of events; transport-type events and collision-type events. An event only depends on the current state of the neutron and is not dependent on events that occurred before. The independence of earlier events means that this process is Markovian. In figure 4.1 the flowchart of the different events a neutron can experience during its 'lifetime' is displayed. The grey boxes represent that a random variable is selected, the circles mean that a direction is imposed on the neutron as a result of the variable selected and the white boxes represent a calculation.

The 'life' of a neutron [17] starts in the 'emission' box and ends in the 'end of story' box. Between these boxes there are many possible paths. At the beginning a position, energy and angle is selected for the neutron out of the possible values. Next, the optical path is selected. After this it is examined if the neutron stays in the the homogeneous medium or leaves it. If it stays in the medium the interaction between the neutron and the medium is calculated. There are two main interactions: absorption and scattering. If the neutron is absorbed its 'life' is terminated. If it scatters it is calculated whether it scatters elastically of inelastically. If inelastically the excitation energy has to be chosen. In both cases the scattering angle is chosen randomly and the energy of the neutron after collision is calculated, after which a new optical path is chosen.

If it leaves the medium it has to be examined whether the interface crossed is a internal interface or a interface at the surface of the geometry. When the neutron crosses an interface at the surface it either leaks from the geometry and is terminated or it reflects back. This reflection can be specular or isotropic. For isotropic reflection the angle of reflection is chosen randomly, while for specular reflection it is calculated. After this a new optical path is selected. If it crosses an internal interface the neutron is repositioned at the interface with its velocity and a new optical path is selected as if the point is an emission point. This is equivalent to using the remainder of the optical path due the the Markovian nature of the process and much simpler.

It is unconfirmed but very plausible due to the description of the flowchart in *Neutron Physics* [17] that *'Limit crossed'* and *'Interface crossed'* are in the wrong position in the flowchart and should be switched.

4.1.3. Serpent input

In table 4.1 the list of materials used in the simulations is shown. For boron the density was chosen at random, as its only purpose was to absorb neutrons escaping the geometry and will not be part of a real life setup.

Table 4.1: List of materials used in the simulations

Material	ID	Density (g/cm^3)	Temperature (K)
Molybdenum	42099.12c	5.03	1200
Graphite	6012.12c	2.27	1200
Holmium	67165.12c	0.14	1200
Beryllium	4009.12c	1.74	1200
Boron	5010.12c	10.0	1200
Tungsten	74184.12c	19.0	1200

The lowest temperature of isotopes that the database of Serpent has information on is 300 K and increases with steps of 300 K. It is therefor almost impossible to create a material at the right temperature. Fortunately, the molybdenum core reaches a temperature of 900 ^{o}C, which is very close to 1200 K. The influence of the temperature on the results was studied by running multiple simulations with different temperatures of the materials. This showed that the influence was very small and could be ignored. The densities of the materials at 1200 K were determined using linear interpolation. This result deviates from reality, but the

difference is very small and the impact on the final results were most likely minimal. Serpent is unable to simulate the damage caused by the gamma radiation in the microspheres, so it was not necessary to model the microspheres as no self-shielding occurs [20] and only the holmium isotopes were modeled.

To check if the output was reliable, the neutron balance had to be correct, meaning that the sum of neutrons absorbed in all materials had to be equal to the number of neutrons emitted by the source. This was done by placing detectors in each material in the geometry to measure not just specific absorption reactions, like n,γ, but all neutron absorption reactions in the materials. It was for this reason the boron sphere is placed around the geometries. It was far easier to measure the neutrons absorbed in this layer than to measure the neutron flux escaping the geometry and it has no impact on the results.

The energy bins necessary for generating the correct neutron spectrum were supplied by S. Brandenburg and H. Beijers of Groningen.

In appendix A an input file is located with some explanation of the input lines.

4.1.4. Serpent output

The output files of Serpent are all written in MATLAB m-file format to simplify post-processing of multiple files. The main output file contains all results calculated by default during the transport cycle. These results are not very interesting for this thesis, as the data measured by the detectors is the focus of this research.

The results for each detector are written in a 12-column vector, where the last two values are the mean value and the relative statistical error. The mean value of the detectors used in this research project is the integral microscopic capture-rate of each material/cell with unit 10^{-24}cm^3. By multiplying the integral microscopic capture rate with the atomic density of the associated material, the probability that a random neutron generated by the source with a spectrum specified by the energy bins is absorbed by that material is obtained. By multiplying the probability that a neutron is absorbed in a n,γ reaction in the target material with the number of neutrons generated per second in the molybdenum core by the electron beams, the number of medical isotopes produced per second is obtained. This is the number χ specified in chapter 2 and with it is possible to see if secondary medical isotope production using the Lighthouse is feasible.

4.2. Post-processing

Post-processing was done using MATLAB [14]. Due to the fact that the output files of Serpent are MATLAB m-files the calculation of the neutron absorption percentage in the targets was relatively easy. Furthermore, it was also used to generate the plots displayed in the next chapter.

5 Results

Before the neutron absorption in the different geometries was calculated, it was examined how the results varied with the number of neutrons simulated. As could be expected, the relative statistical error decreased with an increasing number of neutrons, while the results stayed (mostly) the same. However, it was also discovered that the neutron absorption could vary a lot between simulations with the same input, with the difference being bigger than the error quite often. This could be solved by increasing the number of neutrons simulated, but as the computation time scaled approximately linear with the number of neutrons, this was very impractical. It was decided to calculate the standard deviation to get a general idea of the variation between simulations and thus the uncertainty of the results.

5.1. Neutron absorption in the spherical geometry

In figure 5.1 the neutron absorption in the holmium layer in the spherical geometry displayed in figures 3.1 and 3.2 can be seen. This simulation was run with 10^6 neutrons started from a point source in x=0, y=0, z=0. A point source was used because the volume of the target was so small that generating neutrons in the molybdenum failed most of the time, but because the geometry was spherical the use of a point source had no effect on the results. The moderator and reflector were made of graphite. The radius of the moderator was increased from 7 cm to 10 cm in steps of 5 mm, with the radius of the holmium target increasing according to equation 3.1, which keeps the target volume constant. At each value of R_2 the simulation was run five times in order to get a more accurate result by averaging the values. R_4 was kept constant at 40 cm, as this was so large that the small decrease in distance between R_3 and R_4 as R_2 became larger had negligible effect on the results. R_5 was kept constant at 60 cm, as this was more than enough to absorb all neutrons escaping the reflector.

It is easy to see that the mean absorption in the holmium target is highest at a moderator radius of 8 cm. At this point, the moderator layer is around 5.7 cm thick and the target 0.18 cm. The fact that this position is optimal is likely due to the fact that if R_2 is decreased the neutron flux in the target increases, but this increase is not enough to counteract the decrease in absorption due to the thinner moderator slowing down less neutrons. The opposite happens when R_2 is increased. The moderator slows down more neutrons, but because the neutron current through the target decreases the total absorption is lower. Due to the relatively high standard deviation a final conclusion of the optimal moderator radius can not be made. The only thing that can be said is that the optimal moderator radius lies between approximately 7 and 9 cm. The decision was made at this point to skip the spherical geometry for the lutetium target due to time constraints.

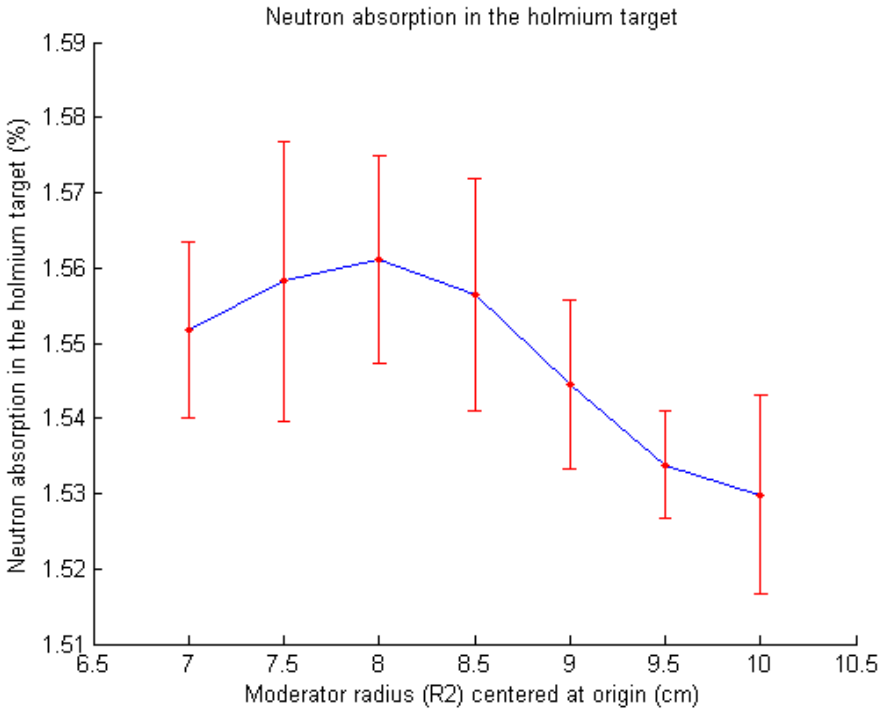

Figure 5.1: Neutron absorption in the holmium target in the spherical geometry

5.2. Neutron absorption in the cylindrical geometry

In the following section all data points are the average of five measurements unless stated otherwise. In each simulation 10^5 neutrons ware generated. The geometry can be seen in figures 3.4 to 3.8.

5.2.1. Holmium target

In the cylindrical geometry it is important that the holmium layer lies in the low photon flux zone, meaning there is a constraint on the width W of the target. In figure 5.2 the neutron absorption can be seen for a holmium target with a width of 1 cm, which lies in the low flux zone for every R_2. The moderator and reflector were made of graphite. For the first six points five calculations were made per point, for the last five three calculations per point. R_4 and R_5 were again kept constant at 40 and 60 cm.

The highest neutron absorption is surprisingly at $R_2 = R_1$, which means there is no moderator at this point. Here, the target is approximately 5.3 cm thick. Apparently, the higher neutron flux far outweighs the effect of the moderator in this setup. It should also be noted that the absorption is about a factor 100 lower than in the spherical setup. This is not surprising, as the target now only surrounds a small portion of the core instead of the entire core and many neutrons escape through the sides of the cylindrical geometry.

In order to see if the absorption could be increased by changing the width of the target W was chosen in such a way that the lower surface of the target fits perfectly between the planes marking the low flux zone:

$$W = 2R_2 \cdot \tan(30^o) \tag{5.1}$$

A visualization of this can be seen in figure 5.3.

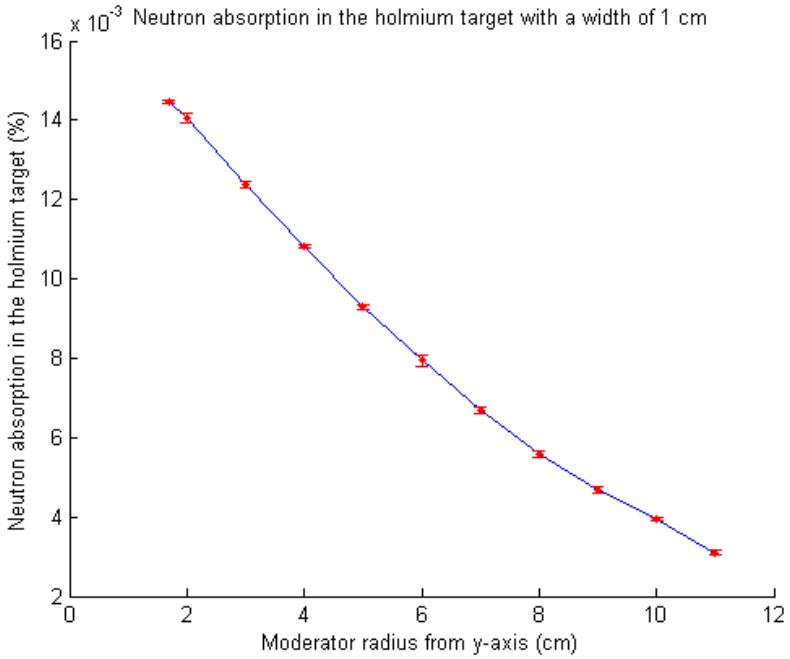

Figure 5.2: Neutron absorption in the holmium target in the cylindrical geometry. The target width is kept constant at 1 cm

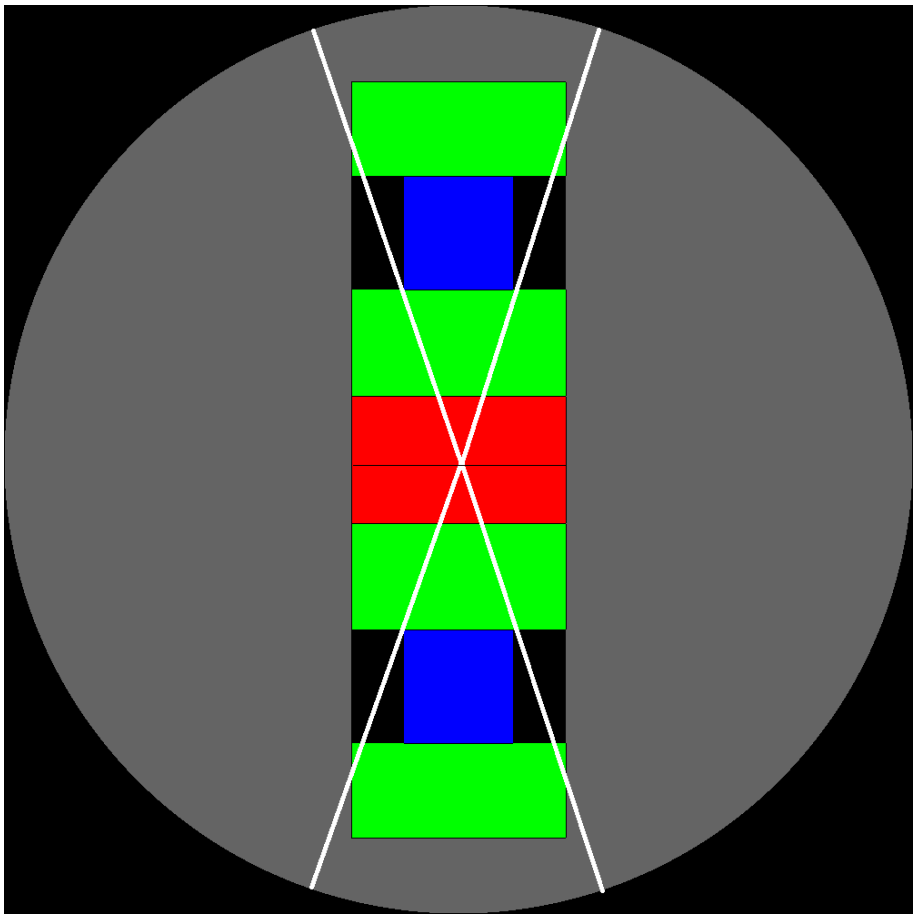

Figure 5.3: Visualization of the low photon flux zone where the holmium target should be placed.

The results of these simulations can be seen in figure 5.4. At R_2=2.5 cm the absorption is the highest. At this point, the target is 2.9 cm wide and 2.2 cm thick. The highest absorption here is around 50% higher than in figure 5.2. From this graph it can be concluded that there is a optimal balance between the moderator radius and target width in the cylindrical geometry. The target thickness is also of importance, but is in this case coupled to the moderator radius and target width because of the constraint of constant volume.

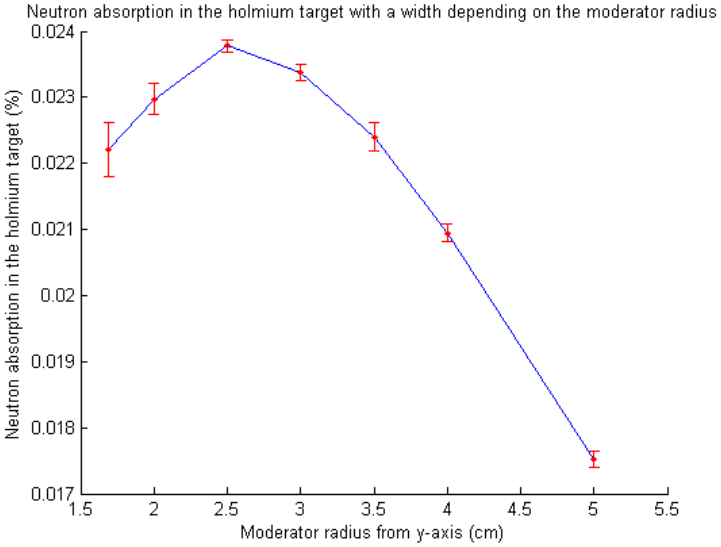

Figure 5.4: Neutron absorption in the holmium target in the cylindrical geometry. The target width is dependent on the moderator radius

The standard deviation in figures 5.2 and 5.4 appears to be much smaller than in figure 5.1, but this is not the case. In figure 5.1 the absorption only changes relatively little with varying moderator radius, while in figures 5.2 and 5.4 the relative change is much higher. This results in a larger difference between the top value of the vertical axis and the bottom value, which makes the standard deviation appear much smaller.

5.2.2. Lutetium target

The lutetium layer suffers no negative effect from the photon flux, so the width of the lutetium target has no constraints, except that it was decided that it should not be wider than the molybdenum target. In figure 5.5 the neutron absorption in lutetium targets of five different widths can be seen. The moderator and reflector were made of graphite. R_4 and R_5 were kept constant at 40 and 60 cm. Just like in figure 5.2 the absorption is highest when there is no moderator. In figure 5.6 the highest absorption for each target width is shown. It is clear that the absorption is highest when the target is 3 cm wide. Unlike in the holmium target the maximum absorption in the lutetium target only depends on the target width (and indirectly on the thickness) as the absorption is highest when there is no moderator.

The results from figure 5.5 suggest that for every width of the holmium target the absorption would be highest when placed directly on the molybdenum target, but this is of course not possible due to the low flux zone constraints.

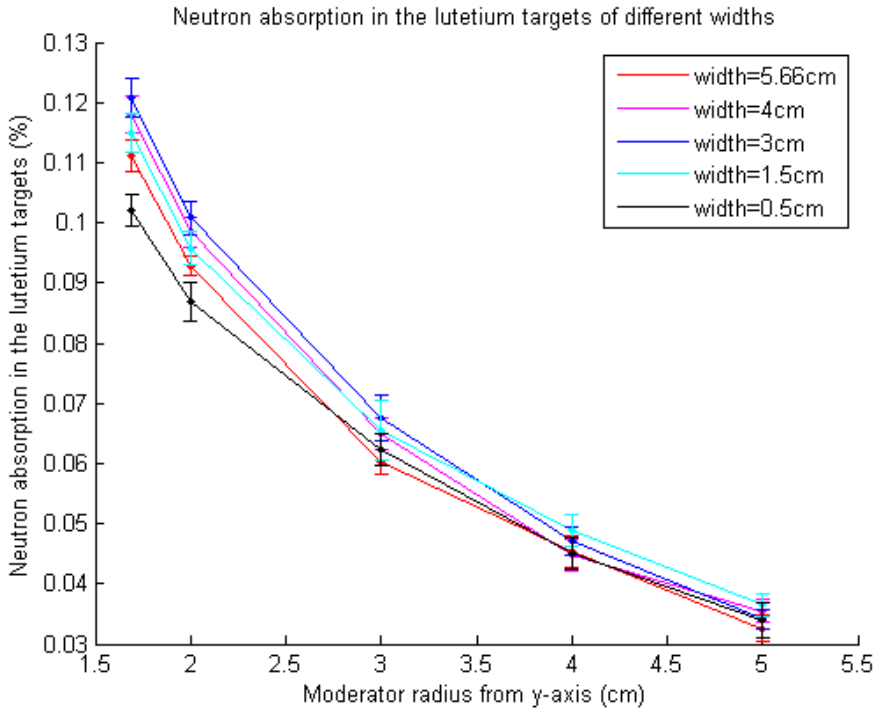

Figure 5.5: Neutron absorption in the lutetium target in the cylindrical geometry. Five different widths for the target were tested

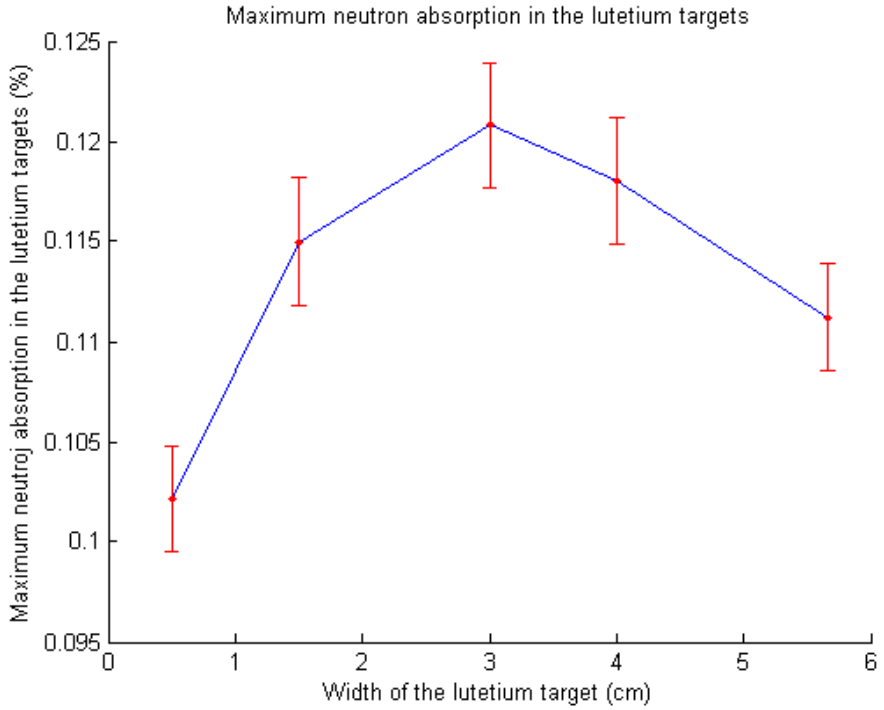

Figure 5.6: Maximum absorption of each lutetium target width in the cylindrical geometry.

5.3. Neutron absorption in cylindrical geometry with added reflector panels

Two reflector panels were placed on both sides of the geometry in order to increase neutron absorption, as shown in figure 3.9. The effect of the panels was tested on the holmium target. By coupling the radius of these panels, which is equal to R_4, with the width of the panels, which is the distance between the plane perpendicular to the y-axis at y=0 and the outer surfaces of the panels, it was easier to examine the influence of the size of the panels on the absorption. This means that if the radius of the reflector layer is 20 cm, the total length of the geometry parallel to the y-axis is 40 cm. The effect of the reflector panels can be seen in figure 5.7. R_2 is kept constant at 2.5 cm and W, the target width, is kept constant at 2.89 cm. Each point is the average of 5 measurements. After 45 cm, increasing the radius and the width only gives a very small improvement. This is to be expected. When the reflector reaches a certain size, all neutrons are either reflected inward or absorbed. At that point, increasing the size has no further effect.

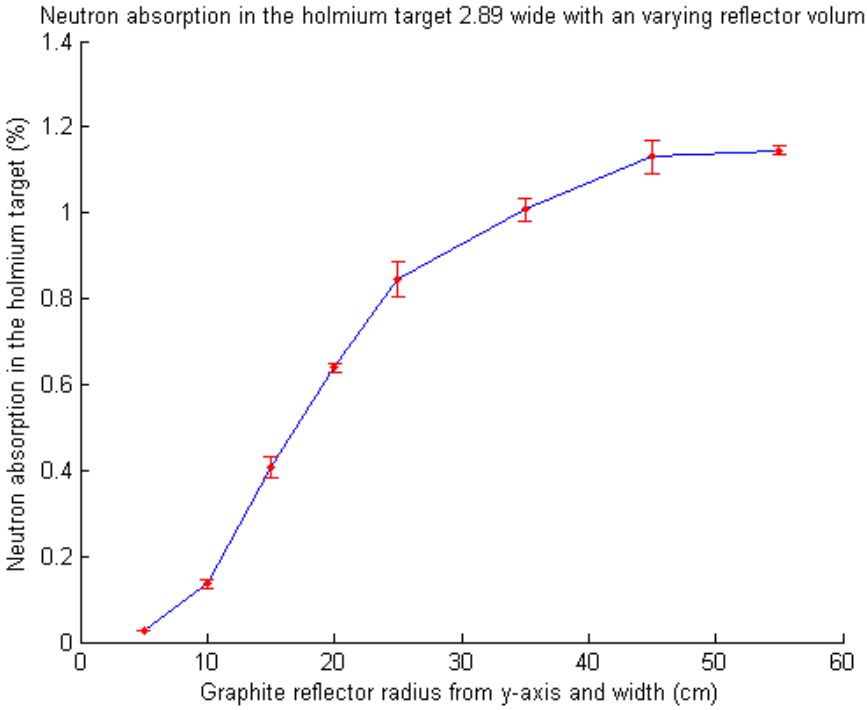

Figure 5.7: Neutron absorption in the holmium target 2.89 cm wide with increasing reflector panel radius and width

By introducing these reflector panels the absorption is increased almost fifty times. The question is now if the moderator between the molybdenum target and the holmium target still has a noticeable effect. In figure 5.8 is shown how the absorption changes as the moderator thickness is varied. W is kept constant at 2.89 cm, which means that if there is no moderator or if the moderator is very thin, part of the target lies outside of the low flux zone, but that is not of importance for what was being examined. R_2 is 45 cm and the total length of the setup 90 cm. R_5 is 65 cm. Unlike the situation from figure 5.2, where the width of the target was also kept constant, the absorption here is not highest when there is no moderator between the core and the target. The reflectors have shifted the optimal position of the target. The moderator thickness still has influence on the absorption of the neutrons in the target, but compared to the effect of the reflector panels it is very small. The difference between the absorption with no moderator and the absorption with optimal moderator thickness is only around 0.20%.

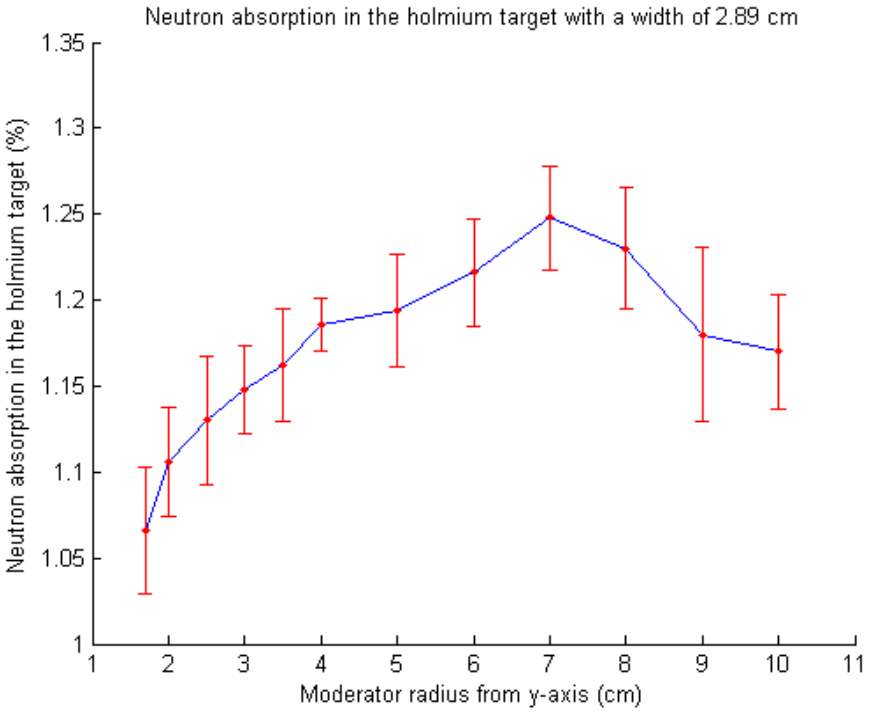

Figure 5.8: Neutron absorption in the holmium target with added reflector panels

5.4. Tungsten gamma-shield

The absorption in the holmium target with the graphite moderator replaced with a tungsten gamma-shield can be observed in figure 5.9. The rest of the parameters were kept the same as in figure 5.8. One thing that is noticeable is that when there is a very small gamma-shield between the target and the core the absorption is higher than when there is no gamma-shield. This is likely due to the reflector panels reflecting the neutrons in such a way that the thermal neutron flux is higher a small distance away from the molybdenum target.

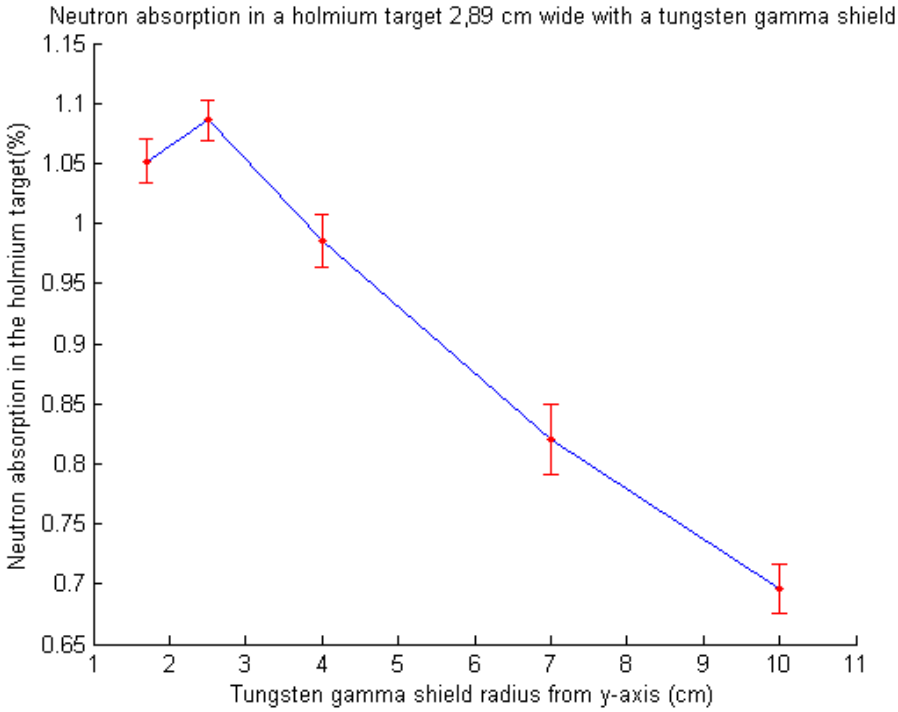

Figure 5.9: Neutron absorption in the holmium target with a tungsten gamma-shield

In figure 5.10 the absorption dependence on both the moderator and gamma-shield radius is plotted. As was expected, when there is no moderator or gamma-shield the absorption is almost the same. Although the effect of the moderator on the absorption is small compared to that of the reflector panels the difference in absorption when using a graphite moderator or tungsten gamma shield can become very large.

The attenuation factor of the tungsten gamma shield for multiple photon energies can be seen in figure 5.11. To calculate the attenuation factor using equation 2.17 the linear attenuation coefficient was determined from table A3.6 of *Principles of radiation shielding* [5] which takes into account Compton Scattering, the Photoelectric effect and Pair Production. Furthermore, only the shortest distance between the molybdenum core and the holmium target was taken into account, which is equal to the thickness of the shield, meaning that the angle θ between the normal of the shield and the incoming photons is zero. Finally, the buildup factor was ignored, as the relation between the photon energy and the absorption in the microspheres was unknown.

From figure 5.11 it can be concluded that a tungsten shield with a thickness of 8 cm stops almost all photons if the buildup factor is negligible (which is almost never true).

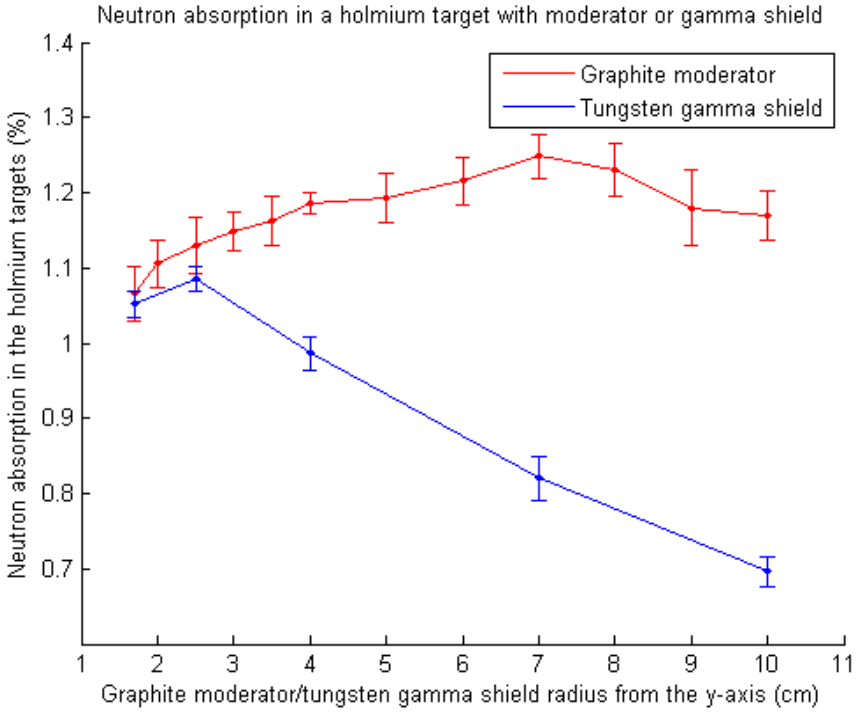

Figure 5.10: Neutron absorption in the holmium target with a graphite moderator or a tungsten gamma-shield

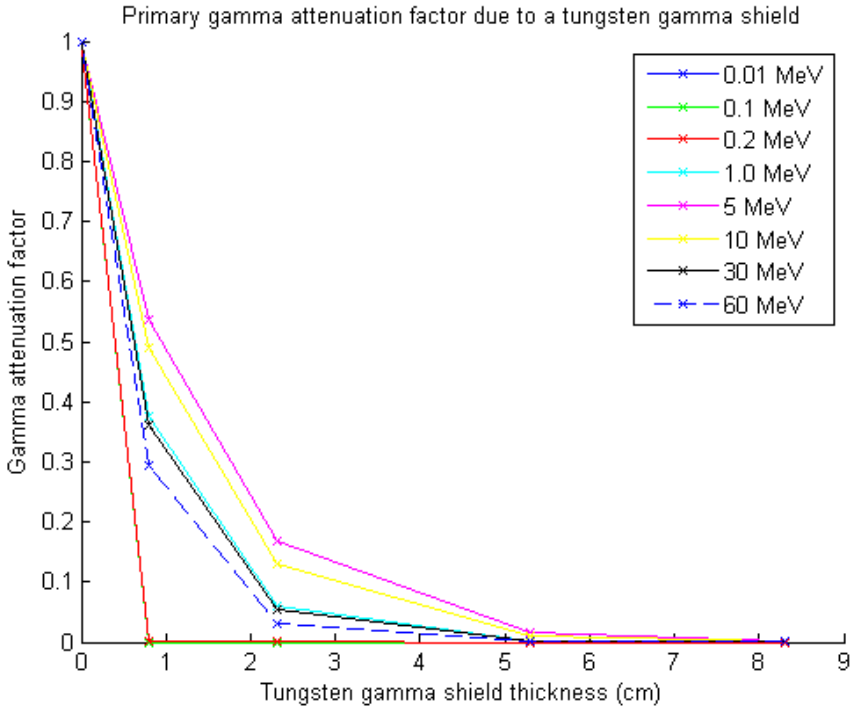

Figure 5.11: Neutron absorption in the holmium target with a graphite moderator or a tungsten gamma-shield

The absorption in both the lutetium target and the holmium target in the cylindrical geometry without reflector panels was too low for the required specific activity to be reached in the radiation time limit, but for lutetium it was even impossible. In order for 20 g of lutetium to reach the required SA more than 600 % of the neutrons would have to be absorbed. This

means there are not enough neutrons being generated in the allowed time. Only if the target is 3 g or lighter it becomes theoretically possible, as at 3 g 99.93% of the neutrons would have to be absorbed. However, if the target becomes smaller, the absorption likely decreases. It is therefore very unlikely that the production of ^{177}Lu will be possible using this setup. Therefore, it was decided to discontinue the research into the neutrons in the lutetium target.

5.5. ^{166}Ho production

Using equation 2.16 the neutron absorption necessary to reach the average required specific activity and the maximum required specific activity in 20g holmium within the irradiation time limit can be calculated. For the average SA this is around 0.21% and for the maximum 0.26%. In figures 5.12 and 5.13 the production rate of ^{166}Ho can be seen for different neutron absorption rates, along with the number of ^{166}Ho atoms necessary in the microspheres to get the average required specific activity of 5.9 $\cdot 10^3$ Ci$\cdot$g^{-1} and the upper limit of the interval of the required specific activity 7.4 $\cdot 10^3$ Ci$\cdot$g^{-1}. In figure 5.12 the production rates are plotted slightly longer than the allowed radiation time, which is approximately $2.9 * 10^5$ s.

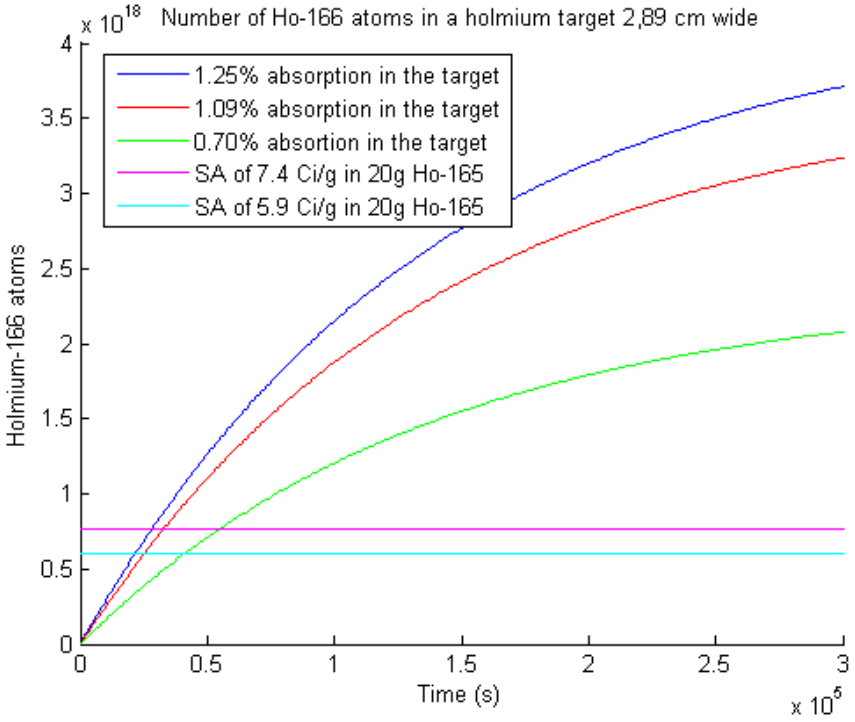

Figure 5.12: ^{166}Ho production for three different absorption rates. The ^{166}Ho atoms needed for the required specific activities are also displayed.

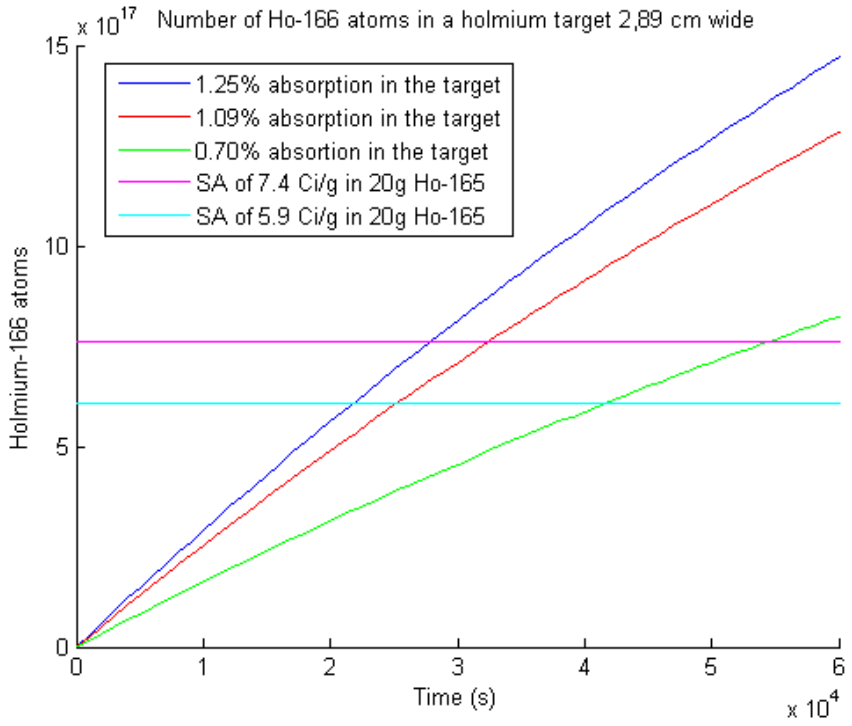

Figure 5.13: ^{166}Ho production for three different absorption rates. The ^{166}Ho atoms needed for the required specific activities are also displayed.

The required specific activity of the holmium microspheres is easily reached, even when using a tungsten gamma-shield instead of a graphite moderator. This means that the geometry can be changed quite drastically with the target specific activity still possible to be reached within the radiation time limit.

In the end beryllium was not used as a moderator. This was because it was not clear how Serpent handles the extra neutrons generated in n,2n reactions. This made it impossible to use beryllium and get reliable results.

A week before the end of this research project new data was supplied by Beijers and Brandenburg. This data was generated using a new version of FLUKA [3, 9]. According to the new calculations the number of neutrons produced by an incident electron is $1.124 * 10^{-2}$. This is around 13% lower than the value used in this research project. As the number of ^{166}Ho atoms produced is linearly dependent on the number of neutrons absorbed per second the production is expected to be 13% lower. Using equation 2.16 the new minimum neutron absorption for the average and maximum required SA are 0.24% and 0.30%. Fortunately, the absorption in the holmium target is still higher than these values, meaning that ^{166}Ho production is still possible.

6

Conclusions & Recommendations

6.1. Conclusions

The goal of this thesis was to investigate if it is possible to use the neutrons that are emitted during the production of ^{99}Mo using ASML's Lighthouse accelerator to produce a second type of medical isotope. The medical isotopes studied in this research project were ^{166}Ho and ^{177}Lu. Using the neutron spectrum supplied by Beijers and Brandenburg the neutron absorption in these two isotopes was simulated. This was first done in a spherical geometry. These results showed that the neutron absorption in a holmium target was high enough, approximately 1.56%, for the production of radioactive holmium loaded microspheres with the required specific activity within the allowed irradiation time frame. The neutron absorption in a lutetium target was not studied in the spherical geometry due to time constraints.

This was repeated in the cylindrical geometry, which resembled the geometry used in the simulations of Beijers and Brandenburg more closely. In this case, the neutron absorption in both targets was too low for the production of the desired medical isotopes. There was, however, a large difference between the two. The required specific activity of ^{177}Lu was on average more than 3000 times higher than that of ^{166}Ho. As a result, this meant that even if 100% of all neutrons that are emitted by the molybdenum target in the allowed radiation time are absorbed in the lutetium target, the specific activity would still not be high enough, even when ignoring radioactive decay of the ^{177}Lu atoms. There are simply not enough neutrons produced in the allowed time frame for the quantity of lutetium tested in the simulations. The only solution is to decrease the quantity of lutetium, but this also decreases the absorption rate in the lutetium target, so it is very unlikely that this will make ^{177}Lu production viable in this setup.

On the other hand, the absorption rate in the holmium target was only around a factor 10 too small. One way to try to increase the absorption rate was to place reflector panels on both sides of the geometry. This proved to be very effective, increasing the absorption rate approximately fifty times to 1.25%, well over the average required absorption which was around 0.21% of the neutrons emitted by the molybdenum target during the maximum irradiation time allowed. Because the absorption was much higher than the required absorption, it was decided to see if the absorption would still be high enough if the moderator was replaced with a gamma shield. An almost 1 cm thick tungsten gamma shied resulted in a neutron absorption of around 1.09%, while a shield with a thickness of around 8.5 cm resulted in a neutron absorption of roughly 0.70%. In both of these situations the absorption is still high enough for the production of ^{166}Ho. Furthermore, calculations showed that if the buildup factor was ignored a tungsten shield with a thickness of 8 cm absorbed almost all gamma radiation.

It can be concluded that the production of 20 g ^{166}Ho with a specific activity of 4.4 to 7.4

$Ci \cdot g^{-1}$ in the cylindrical geometry is possible using the Lighthouse ^{99}Mo production facility. However, in this thesis certain assumptions were made and certain aspects ignored that could have a very big influence on the final results. These are discussed in the next section.

6.2. Recommendations

Because of the nature of the Monte Carlo method a simulation always returns a result. The statistical fluctuations of these results decrease as more neutrons are simulated. Besides statistical fluctuations it is possible that there was a systematic deviation in the results. Validation of the results is therefore very important and recommended for future research. There are multiple options for validation:

- An analytic calculation
- A literature study
- An experiment
- Analysis using a different package

A drawback of Serpent is that it can not simulate the damage done due to gamma radiation to the microspheres. Because of this only the holmium atoms were modeled in order to speed up calculation time. Fortunately, the microspheres have no major influence on the absorption of neutrons in the holmium atoms, as no self-shielding occurs. It is, however, less fortunate that the photon absorption in the microspheres can not be simulated. The gamma dose rate has a large influence on the integrity of the microspheres and a limiting factor on how long they can be irradiated. It is possible that the time it takes for the microspheres to start disintegrating is shorter than the time required for the production of the isotopes, making production not viable. One way to see if this would be a problem is to do an in depth analysis of the gamma spectrum of the reactor in Delft and the gamma spectrum that is emitted from the molybdenum target. A second option would be to use an other program that is capable of simulating both photons and organic molecules.

In order to minimize the effect of the photons, the graphite moderator was replaced with a tungsten photon shield. Results showed that even with this shield the neutrons absorption was still well above target, but the effect on the photon flux was not studied using simulations. This is because the photons are not emitted isotropically, but have a forward bias. In Serpent, if there is no input given for the direction in a source term the particles are emitted isotropically, but if a direction has to be specified it is done in the form of a pencil beam. This means that in order to simulate a photon spectrum that is practically the same as the real life spectrum thousands of pencil beams would have to be specified manually. Because of this, it might be more practical to study the effect of the tungsten shield with another program, if no easier way of simulating the correct photon spectrum in Serpent can be found. It would also be very useful to determine the buildup factor regarding the gamma attenuation due to the tungsten shield, as the results of the simulations can then be validated.

One thing that was ignored during this research was the temperature of the target. Because graphite is a very good heat conductor and the core reaches a temperature of 900 °C, the target is likely to become very hot as well. For lutetium this is not a problem, as its melting point is much higher, but this is very problematic for the holmium loaded microspheres. Because they are made of organic molecules they can not sustain high temperatures, with a complete structural disintegration as a result. There are several possible options which can be combined to prevent this:

- Increased cooling of the core
- Placing an isolator between the core and the target
- Cooling of the target

It is recommended that an analysis of the heat transport through the setup is done to see what value the temperature of the target would reach without the measures mentioned above and to see if they could be implemented without effecting the neutron absorption rate too much.

Another thing that was ignored during this project was change in neutron absorption in the due to the increasing number of radioactive atoms/decreasing number of stable atoms. For holmium only a very small fraction of the ^{165}Ho atoms needs to become radioactive to reach the required specific activity, so the effect is expected to be minimal, but it might prove useful to study if and how the absorption changes during the irradiation time. At the moment Serpents database contains no information of ^{166}Ho, which makes it impossible to simulate a material containing both isotopes. This information might be added in the future and otherwise another program will have to be used.

In this research project beryllium was not used as a moderator because it was not clear how Serpent handled the n,2n reactions. This is unfortunate as the increased neutron flux due to the n,2n reaction could be of use in making sure isotope production is viable in certain time frames. It is therefore very useful for future research to find out how this is handled in Serpent and to study if beryllium works better as moderator than graphite in this setup.

At the moment research is being done on the separation of ^{176}Lu and ^{177}Lu. By separating these two isotopes the specific activity per gram becomes much higher. This might make the production of ^{177}Lu viable and should be taken into account in future research.

Something that also could be useful for the isotope production is to use a different material than molybdenum for the electron beam target. There might be another element that can be turned into a medical isotope using electron beams while emitting neutrons at a higher rate than ^{100}Mo.

Furthermore, there are many more medical isotopes that can be produced using neutron capture. It is possible that these can be produced using the Lighthouse accelerator, with some even being better candidates than ^{177}Lu and ^{166}Ho. This is worth investigating in future research.

Finally, the simulations should be repeated with the new neutron spectrum supplied by H. Beijers and S. Brandenburg to see if the absorption changes and if so, by how much.

At the moment it is not possible to recommend a final configuration for the production facility. This is because there are still many unknown factors, such as how the different targets should be inserted in and extracted from the setup, what precautions are necessary to prevent the microspheres from becoming to hot, if additional gamma shielding is necessary to protect the microspheres and manufacturing constraints. One recommendation that could be made is that the cylindrical geometry would be a good starting point for designing the final configuration. One change that could be made is replacing the reflector panels with a spherical reflector layer. This might be more efficient as the neutrons are emitted isotropically.

Bibliography

[1] D. Bakker, N. Klotz, Y. van Knippenberg, C. Smeets, and E. Zwiers. The use of 'new' radioactive isotopes in cancer therapy. Radboud University, June 2017.

[2] J.P.M. Beijers and S. Brandenburg. Shielding considerations for the 99mo facility. University of Groningen, March 2, 2016.

[3] TT Böhlen, F Cerutti, MPW Chin, Alberto Fassò, Alfredo Ferrari, PG Ortega, Andrea Mairani, Paola R Sala, G Smirnov, and V Vlachoudis. The fluka code: developments and challenges for high energy and medical applications. *Nuclear Data Sheets*, 120: 211–214, 2014.

[4] World cancer day. Myth 2 - cancer is a disease of the wealthy, elderly and developed countries. URL `http://www.worldcancerday.org/myth-2-cancer-disease-wealthy-elderly-and-developed-countries`. Online; last accessed September 4, 2017.

[5] Arthur B Chilton, J Kenneth Shultis, and Richard E Faw. Principles of radiation shielding. 1984.

[6] Patrick de Jager. personal communication.

[7] E. de Sanctis, S. Monti, and M. Ripani. *Energy from nuclear fission: an Introduction*. Springer, Cham, 2016.

[8] James J Duderstadt and Louis J Hamilton. *Nuclear reactor analysis*, volume 1. Wiley New York, 1976.

[9] Alfredo Ferrari, Paola R Sala, Alberto Fasso, and Johannes Ranft. Fluka: A multi-particle transport code (program version 2005). Technical report, 2005.

[10] RA Forrest, J Kopecky, and J-Ch Sublet. The european activation file: Eaf-2003 cross section library. *UKAEA FUS*, 486, 2002.

[11] G. Kolata. As other death rates fall, cancer's scarcely moves. *The New York Times*, 24, 2009.

[12] J. Leppänen, M. Pusa, T. Viitanen, V. Valtavirta, and T. Kaltiaisenaho. The serpent monte carlo code: Status, development and applications in 2013. *Annals of Nuclear Energy*, 82:142–150, 2015.

[13] Ivan Lux and László Koblinger. *Monte Carlo particle transport methods: neutron and photon calculations*, volume 102. CRC press Boca Raton, Florida, 1991.

[14] MATLAB. *8.0.0.783 (R2012b)*. The MathWorks Inc., Natick, Massachusetts, 2010.

[15] Robert McNeel et al. Rhinoceros 3d, version 4.0. *Robert McNeel & Associates, Seattle, WA*, 2010.

[16] Nucleair Nederland. Medische isotopen: belang voor de wereld en kansen voor nederland. Downloaded from https://nucleairnederland.nl/downloads.

[17] Paul Reuss. *Neutron physics*. EDP sciences, 2012.

[18] X-5 Monte Carlo Team. Mcnp - version 5, vol. i: Overview and theory. LA-UR-03-1987 (2003).

[19] Cancer Research UK. Worldwide cancer statistics. URL http://www.cancerresearchuk.org/health-professional/cancer-statistics/worldwide-cancer#heading-Zero. Online;last accessed September 4, 2017.

[20] M.A.D. Vente. Preclinical studies on holmium-166 poly(l-lactic acid) microspheres for hepatic arterial radioembolization. PhD thesis, Utrecht University, 2009.

A

Serpent input

A.1. Serpent input lines

The Serpent code has no interactive user interface. All communication between the code and the user is handled through one or several text based input files and various output files. An example can be seen in appendix A. Every line contains a command or input card as they are called in Serpent, or a number of parameters associated with that command. In this section a brief description of the different input cards will be given using a number of examples from the code located in appendix A. For a more detailed description of all input cards it is recommended to read the manual of Serpent, which can be found on the website, or to read the on-line wiki. Just like in MATLAB, everything written after a %-sign on the same line is seen as a comment.

set acelib ”home/jblokker/SERPENT_calculations/Holmium-sigaar/sss_jeff311u.xsdata”
Set acelib is used to define a path to the directory where Serpent's database is located, which has contains the properties of a very large number of isotopes.

mat molybdenum -5.03 rgb 255 0 0
42099.12c -1
mat is the input card that defines a material used in the simulations. This is done by using different parameters. 'Molybdenum' is the name of this material, '-5.03' the mass density in g/cm^3. The minus sign is used to indicate it is the mass density and not the atomic density. rgb stands for red, green, blue and is used to give the material a certain color in the plots (if these are generated). '42099.12c' is the ID of a certain isotope at a certain temperature, in this case ^{100}Mo at 1200 K, '42' being the atomic number and '099' the mass number. '-1' indicates the mass fraction of this isotope, as a material can consist of multiple isotopes. Again, the minus sign is used to indicate it is a mass fraction instead of atomic fraction.

surf 1 cyly 0 0 1.693 -2.83 2.83
surf is used to define a surface. Surfaces are used to create geometries used in the simulations. '1' is the name of the surface, as it is better to use numbers as names for surfaces (and cells) as the code becomes very cluttered if normal names are used. 'cyly' defines the surface as a cylinder parallel to the y-axis. The two zeros are the x and z coordinates of the axis of the cylinder and '1.693' is the radius in cm. '-2.83' and '2.83' are the ends of the cylinder in cm.

cell 3 0 holmium 2 -3 4 -5
cell is the input card to define a cell. Cells are used to fill the different volumes of the geometry created by the intersection of surfaces. '3' is the name of the cell. '0' is the universe number of the cell. In this research this number was not of importance, but it had to be defined. 'holmium' is the material of the cell. '2 -3 4 -5' are surface names, used to determine

the cell shape. Positive entries refer to positive/outside surface sides and negative entries to negative/inside surface sides. In this case, '2' and '3' are cylinders parallel to the y-axis and '4' and '5' planes perpendicular to the y-axis, which means that cell 3 is a holmium ring between the outer surface of cylinder '2' and the inner surface of cylinder '3' and between the positive surface (normal vector parallel to the y-axis in the positive direction) of plane '4' and the negative surface (normal vector parallel to the y-axis in the negative direction) of plane '5'.

det target dc 3 dr 102 holmium
det is the detector input card. Detectors are mainly used to see how many reactions of certain type occur within a certain cell, material, universe etc. 'target' is the name of this detector. 'dc 3' defines the cells where the reactions are monitored, with '3' being the cell name. 'dr 102 holmium' defines which reaction is measured, with '102' being the n,γ reaction and 'holmium' the material in which the reaction occurs.

plot 1 1000 1000
The input card *plot* is used to generate a 2D overview of the geometry. '1' is the orientation of the plot, in this case the yz-plane. If no parameter is given for the position on the axis perpendicular to the plane the zero position is assumed. '1000' and '1000' are width and the height of the plot in pixels.

set nps 100000 [20]
set nps defines the total amount of neutrons simulated, 100000 here, and in how many batches the simulation is run, 20 in this case.

src NeutronSource1 sc 1 sb 301
0.00000000020000 0.0000000000
0.00000000029297 0.0000000000
3.16640000000000 0.0038682946
src defines a neutron source. 'NeutronSource1' is the name of the source. 'sc 1' defines in which cell the neutrons are started and 'sb 301' is used to define an energy spectrum for the neutrons using a number of energy bins, in this case 301. The first two bins and a random one are shown. The first column contains the upper boundary of the energy bin in MeV and the second column the bin weight. The code samples the energy bin according to the probability calculated from the bin weights, and the energy uniformly between the bin boundaries. The weight of the first bin must be set to zero. By default the neutrons are emitted isotropically.

A.2. Serpent input file

```
set acelib "home/jblokker/SERPENT_calculations/Holmium-sigaar/sss_jeff311u.xsdata"
  % — materials in the layers:
  mat molybdenum -5.03 rgb 255 0 0 % molybdenum with 50% density with red color in plot 42099.12c -1
  mat graphite1 -2.267 rgb 0 255 0 % graphite moderator or reflector 6012.12c -1
  mat graphite2 -2.267 rgb 0 255 0 % graphite moderator or reflector 6012.12c -1
  mat holmium -0.13889 rgb 0 0 255 % holmium target 67165.12c -1
  mat beryllium -1.74 rgb 0 0 255 % beryllium moderator/reflector 4009.12c -1
  mat boron -10 rgb 100 100 100 % boron 5010.12c -1
  mat tungsten -19 rgb 255 255 0 % tungsten gamma shield 74184.12c -1
  % — Cylinders parallel to the y-axis centered at x=0, z=0
  surf 1 cyly 0 0 1.693 -2.83 2.83 % molybdenum core
  surf 2 cyly 0 0 7 -2.83 2.83 % moderator
  surf 3 cyly 0 0 8.05 -2.83 2.83 % target
  surf 4 py -1.443375672974064
  surf 5 py 1.443375672974064
  surf 6 cyly 0 0 45 -2.83 2.83 % reflector
```

```
surf 7 py -2.83
surf 8 py 2.83
surf 9 cyly 0 0 0.565 -45 45 % electron beam opening
surf 10 cyly 0 0 45 -45 45 % reflector
surf 11 py -45
surf 12 py 45
surf 13 sph 0 0 0 65
% — cells
cell 1 0 molybdenum -1
cell 2 0 graphite1 1 -2
cell 3 0 holmium 2 -3 4 -5
cell 4 0 graphite1 2 -3 7 -4
cell 5 0 graphite1 2 -3 5 -8
cell 6 0 graphite2 3 -6
cell 7 0 boron 6 -13 7 -8
cell 8 0 boron 10 -13 11 -7
cell 9 0 boron 10 -13 8 -12
cell 10 0 boron -13 -11
cell 11 0 boron 12 -13
cell 12 0 void -9 11 -7
cell 13 0 void -9 8 -12
cell 14 0 graphite2 9 -10 11 -7
cell 15 0 graphite2 9 -10 8 -12
cell 16 0 outside 13
% — detectors
det target dc 3 dr 102 holmium % — n,gamma reactions in target
det target-all dc 3 dr 101 holmium % — all absorption in holmium target
det molybdenum dc 1 dr 101 molybdenum % — all absorption in molybdenum
det graphite1 dm graphite1 dr 101 graphite1
det graphite2 dm graphite2 dr 101 graphite2
det boron dm boron dr 101 boron
det tungsten dm tungsten dr 101 tungsten
% — Geometry plotter
plot 1 1000 1000
plot 2 1000 1000
%set tpa 0 600 0.01 1 1000000
% — Neutron source
set nps 100000 [20]
src NeutronSource1 sc 1 sb 301 0.00000000020000 0.0000000000 0.00000000029297
0.0000000000 0.00000000042917 0.0000000000 0.00000000062867 0.0000000000 0.00000000092092
0.0000000000 0.00000000134900 0.0000000000 0.00000000197610 0.0000000000 0.00000000289480
0.0000000000 0.00000000424050 0.0000000000 0.00000000621170 0.0000000000 0.00000000909940
0.0000000000 0.00000001332900 0.0000000000 0.00000001952600 0.0000000000 0.00000002860300
0.0000000000 0.00000004189900 0.0000000000 0.00000006137700 0.0000000000 0.00000008990900
0.0000000000 0.00000013170000 0.0000000000 0.00000019293000 0.0000000000 0.00000028261000
0.0000000000 0.00000041399000 0.0000000000 0.00000053158000 0.0000000000 0.00000062506000
0.0000000000 0.00000068256000 0.0000000000 0.00000083368000 0.0000000000 0.00000087642000
0.0000000000 0.00000112540000 0.0000000000 0.00000144500000 0.0000000000 0.00000185540000
0.0000000000 0.00000238240000 0.0000000000 0.00000305900000 0.0000000000 0.00000392790000
0.0000000000 0.00000504350000 0.0000000000 0.00000647600000 0.0000000000 0.00000831530000
0.0000000000 0.00001067700000 0.0000000000 0.00001371000000 0.0000000000 0.00001760400000
0.0000000000 0.00002260300000 0.0000000000 0.00002902300000 0.0000000000 0.00003726600000
0.0000000000 0.00004785100000 0.0000000000 0.00006144200000 0.0000096276 0.00007889300000
0.0000000000 0.00010130000000 0.0000000000 0.00013007000000 0.0000112418 0.00016702000000
0.0000000000 0.00021445000000 0.0000000000 0.00027536000000 0.0000304697 0.00035357000000
0.0000102571 0.00045400000000 0.0000000000 0.00058295000000 0.0000109263 0.00074852000000
```

0.0000101236 0.00096112000000 0.0000318992 0.00123410000000 0.0000515308 0.0013639000000
0.0000000000 0.00150730000000 0.0000407604 0.00158460000000 0.0000203164 0.0016659000000
0.0000097893 0.00184110000000 0.0000208697 0.00203470000000 0.0000302071 0.0022487000000
0.0000292336 0.00248520000000 0.0000745924 0.00261260000000 0.0000000000 0.0027465000000
0.0000203186 0.00286350000000 0.0000085819 0.00303540000000 0.0000000000 0.0033546000000
0.0000513589 0.00370740000000 0.0000568893 0.00409740000000 0.0001096646 0.0043074000000
0.0000201352 0.00452830000000 0.0000406237 0.00500450000000 0.0001155168 0.0055308000000
0.0001029637 0.00626730000000 0.0000638752 0.00710170000000 0.0002444185 0.0080473000000
0.0002527441 0.00911880000000 0.0001844750 0.01030000000000 0.0002556228 0.0117000000000
0.0002964011 0.01330000000000 0.0003620280 0.01500000000000 0.0003994185 0.0170000000000
0.0004386867 0.01930000000000 0.0006017977 0.02130000000000 0.0005161435 0.0219000000000
0.0001310075 0.02360000000000 0.0004302428 0.02420000000000 0.0001115377 0.0248000000000
0.0001821993 0.02610000000000 0.0003650148 0.02810000000000 0.0005394978 0.0318000000000
0.0012188755 0.03430000000000 0.0008737354 0.03520000000000 0.0001696830 0.0361000000000
0.0002483720 0.04090000000000 0.0011759340 0.04630000000000 0.0017006329 0.0525000000000
0.0018037794 0.05660000000000 0.0015818483 0.05950000000000 0.0009716712 0.0625000000000
0.0007550271 0.06740000000000 0.0015776703 0.07640000000000 0.0037680938 0.0865000000000
0.0044259948 0.09800000000000 0.0040029871 0.11110000000000 0.0056361036 0.1168000000000
0.0025523576 0.12280000000000 0.0026528929 0.12910000000000 0.0032953261 0.1357000000000
0.0039634607 0.14260000000000 0.0035820392 0.15000000000000 0.0035615307 0.1576000000000
0.0039672866 0.16160000000000 0.0020227942 0.16570000000000 0.0018765653 0.1699000000000
0.0021303417 0.17420000000000 0.0021051154 0.18320000000000 0.0048993140 0.1925000000000
0.0054457184 0.20240000000000 0.0051853406 0.21280000000000 0.0060349118 0.2237000000000
0.0059847821 0.23520000000000 0.0068331503 0.24720000000000 0.0071858718 0.2599000000000
0.0074373715 0.27320000000000 0.0083849959 0.28020000000000 0.0044304074 0.2872000000000
0.0040254027 0.29450000000000 0.0044116711 0.30200000000000 0.0046790905 0.3096000000000
0.0043436794 0.31750000000000 0.0047432153 0.33370000000000 0.0101277488 0.3508000000000
0.0108710165 0.36880000000000 0.0115403482 0.38770000000000 0.0126741035 0.4076000000000
0.0135537126 0.42850000000000 0.0130819894 0.45050000000000 0.0144624620 0.4736000000000
0.0140645926 0.49790000000000 0.0159801502 0.51050000000000 0.0077196543 0.5234000000000
0.0080064026 0.53660000000000 0.0079726210 0.55020000000000 0.0092476760 0.5784000000000
0.0171796909 0.60810000000000 0.0185535972 0.63930000000000 0.0195840181 0.6721000000000
0.0194065718 0.70650000000000 0.0201877112 0.74270000000000 0.0215817914 0.7808000000000
0.0210780176 0.82090000000000 0.0204808731 0.86290000000000 0.0208252974 0.9072000000000
0.0217317758 0.95370000000000 0.0214685403 0.96160000000000 0.0038035654 0.9778000000000
0.0070373310 1.00260000000000 0.0113669390 1.05400000000000 0.0227294654 1.1080000000000
0.0224089354 1.16480000000000 0.0219843786 1.19430000000000 0.0108224652 1.2246000000000
0.0115995674 1.28740000000000 0.0215613006 1.35340000000000 0.0224121041 1.4227000000000
0.0206658422 1.49570000000000 0.0222489755 1.53360000000000 0.0100300007 1.5724000000000
0.0105231771 1.61220000000000 0.0103413181 1.65300000000000 0.0098948857 1.7377000000000
0.0192294717 1.82680000000000 0.0181841286 1.87310000000000 0.0091204768 1.9205000000000
0.0087558493 1.96910000000000 0.0085069667 2.01900000000000 0.0083597227 2.1225000000000
0.0152683053 2.23130000000000 0.0147860668 2.26890000000000 0.0045097654 2.3069000000000
0.0048320088 2.34570000000000 0.0046423103 2.36520000000000 0.0021889447 2.3852000000000
0.0019434597 2.42510000000000 0.0043337567 2.46600000000000 0.0044231723 2.5924000000000
0.0116002950 2.72530000000000 0.0101068355 2.86510000000000 0.0102049943 3.0119000000000
0.0086227411 3.08820000000000 0.0039444428 3.16640000000000 0.0038682946 3.2465000000000
0.0036520671 3.32870000000000 0.0031255902 3.49940000000000 0.0060600207 3.6788000000000
0.0056530384 3.86740000000000 0.0050354501 4.06570000000000 0.0041424562 4.2741000000000
0.0036197172 4.49330000000000 0.0035371906 4.60700000000000 0.0015345234 4.7237000000000
0.0012737055 4.84320000000000 0.0012832291 4.96590000000000 0.0013535915 5.2205000000000
0.0021961447 5.48810000000000 0.0021041472 5.76950000000000 0.0018658974 5.9156000000000
0.0006455593 6.06530000000000 0.0007231321 6.21890000000000 0.0006776174 6.3763000000000
0.0005900685 6.53770000000000 0.0006727426 6.59240000000000 0.0002686152 6.6476000000000
0.0002373806 6.70320000000000 0.0002040021 6.87290000000000 0.0006021732 7.0469000000000
0.0005592231 7.22530000000000 0.0004575107 7.40820000000000 0.0004396441 7.5957000000000

0.0003244821 7.78800000000000 0.0003735580 7.98520000000000 0.0004066942 8.18730000000000
0.0004226581 8.39460000000000 0.0003548305 8.60710000000000 0.0002847004 8.82500000000000
0.0003253200 9.04840000000000 0.0002777003 9.27740000000000 0.0003825945 9.51230000000000
0.0002066602 9.75310000000000 0.0002013805 10.00000000000000 0.0002848327 10.25320000000000
0.0002926057 10.51270000000000 0.0002123598 10.77880000000000 0.0001207896 11.05170000000000
0.0001788718 11.33150000000000 0.0001379710 11.61830000000000 0.0001420741 11.91250000000000
0.0001626494 12.21400000000000 0.0001474896 12.52320000000000 0.0001319570 12.84020000000000
0.0001554459 13.16530000000000 0.0001223462 13.49860000000000 0.0001229542 13.84030000000000
0.0000942384 14.19070000000000 0.0000818584 14.54990000000000 0.0000928069 14.91830000000000
0.0000934761 15.29590000000000 0.0000607155 15.68310000000000 0.0001250249 16.08010000000000
0.0000352417 16.48720000000000 0.0000606167 16.90460000000000 0.0000305866 17.33250000000000
0.0000618306 17.77130000000000 0.0000670903 18.22120000000000 0.0000624092 18.68250000000000
0.0000411012 19.15540000000000 0.0000718128 19.64030000000000 0.0000613972 20.00000000000000
0.0000690430 20.98800000000000 0.0000856467 21.97600000000000 0.0001126632 22.96410000000000
0.0000334858 23.95210000000000 0.0000310904 24.94010000000000 0.0000247647 25.92810000000000
0.0000504755 26.91610000000000 0.0000197092 27.90420000000000 0.0000234191 28.89220000000000
0.0000000000 29.88020000000000 0.0000000000 30.86820000000000 0.0000201325 31.85620000000000
0.0000000000 32.84430000000000 0.0000000000 33.83230000000000 0.0000000000 34.82030000000000
0.0000000000 35.80830000000000 0.0000107040 36.79640000000000 0.0000106221 37.78440000000000
0.0000000000 38.77240000000000 0.0000000000 39.76040000000000 0.0000000000 40.74840000000000
0.0000000000 41.73650000000000 0.0000000000 42.72450000000000 0.0000000000 43.71250000000000
0.0000000000 44.70050000000000 0.0000000000 45.68850000000000 0.0000000000 46.67660000000000
0.0000000000 47.66460000000000 0.0000000000 48.65260000000000 0.0000000000 49.64060000000000
0.0000000000 50.62860000000000 0.0000000000 51.61670000000000 0.0000000000 52.60470000000000
0.0000000000 53.59270000000000 0.0000000000 54.58070000000000 0.0000000000 55.56870000000000
0.0000000000 56.55680000000000 0.0000000000 57.54480000000000 0.0000000000 58.53280000000000
0.0000000000 59.52080000000000 0.0000000000 60.50880000000000 0.0000000000